Computer Modeling in Engineering & Sciences CMES, vol.123, no.2, pp.739-776, 2020

An ADI Finite Volume Element Method for a Viscous Wave Equation with Variable Coefficients

Mengya Su[1], Zhihao Ren[1] and Zhiyue Zhang[1, *]

Abstract: Based on rectangular partition and bilinear interpolation, we construct an alternating-direction implicit (ADI) finite volume element method, which combined the merits of finite volume element method and alternating direction implicit method to solve a viscous wave equation with variable coefficients. This paper presents a general procedure to construct the alternating-direction implicit finite volume element method and gives computational schemes. Optimal error estimate in L^2 norm is obtained for the schemes. Compared with the finite volume element method of the same convergence order, our method is more effective in terms of running time with the increasing of the computing scale. Numerical experiments are presented to show the efficiency of our method and numerical results are provided to support our theoretical analysis.

Keywords: Viscous wave equation, alternating direction implicit finite volume element method, error estimates, L^2 norm.

1 Introduction

We consider in this paper the numerical approximation of a viscous wave equation on a bounded domain $\Omega \subset \mathbb{R}^m$ of the form

$$
\begin{aligned}
&(a) \quad \frac{\partial^2 u}{\partial t^2} + \gamma_1 \frac{\partial u}{\partial t} - \frac{\partial}{\partial t} \nabla \cdot (Q \nabla u) - \nabla \cdot (A \nabla u) = S(X,t), X \in \Omega, t > 0, \\
&(b) \quad u = 0, X \in \partial\Omega, t > 0, \\
&(c) \quad u(X,0) = u_0(X), \frac{\partial u}{\partial t}(X,0) = u_1(X), X \in \Omega,
\end{aligned} \tag{1}
$$

where γ_1 is a nonnegative coefficient, S denotes a source term, u_0 and u_1 are initial data, and $A = A(X)$ and $Q = Q(X)$ are diagonal, nonnegative diffusion tensors:

[1] School of Mathematical Sciences, Jiangsu Provincial Key Laboratory for Numerical Simulation of Large Scale Complex Systems, Nanjing Normal University, Nanjing, 210023, China.
* Corresponding Author: Zhiyue Zhang. Email: zhangzhiyue@njnu.edu.cn.
Received: 08 September 2019; Accepted: 29 November 2019.

$A = diag(a_1, \ldots, a_m); a_l = a_l(X) \geq 0; Q = diag(q_1, \ldots, q_m); q_l = q_l(X) \geq 0.$

Here, we have selected the homogeneous Dirichlet boundary condition for simplicity. Our analysis can be adjusted to accommodate other boundary conditions.

Eq. (1) represents an interesting class of problems including the propagation of acoustic waves and microscale heat transfer. Such problems have been widely concerned and studied because of their realistic physical background. Early work about them can be seen in Sei et al. [Sei and Symes (1995); Harfash (2008); Dai and Nassar (1999); Deng, Wang and Zhao (2010); Lim, Kim and Douglas Jr (2007); Verwer (2009); Zhang and Zhao (2001); Karaa (2010a); Zhang (2011)]. In Sei et al. [Sei and Symes (1995)], the authors gave the dispersion analysis of numerical wave propagation and its computational consequences. A finite-difference scheme had been constructed for solving the heat transport equation at the microscale in Dai et al. [Dai and Nassar (1999)]. Verwer studied the numerical time integration of a class of viscous wave equations by means of Runge-Kutta methods in Verwer [Verwer (2009)]. In Zhang [Zhang (2011)], Professor Zhang proposed a new multistep finite difference fractional step method for solving a viscous wave equation and proved that the new scheme is unconditionally stable in the sense of von Neumann. A Neumann problem for a wave equation perturbed by viscous terms with small parameters was considered and the interaction of waves with the diffusion effects caused by a higher-order derivative with small coefficient e was investigated in De Angelis [De Angelis (2019)]. For other recent development, we can see Deng et al. [Deng (2018); Khelghati and Baghaei (2018); Zhao and Liu (2018); Chen, Zhou, Jiang et al. (2019)].

Finite volume element method discretizes the integral form of conservation law of differential equation by choosing linear or bilinear finite element space as the trial space. The method, also known as the generalized difference method [Li, Chen and Wu (1999)], was proposed by Professor Ronghua Li in the 1980s based on the finite difference method and the finite element method. It has been widely used in computational fluid dynamics because of its attractive properties, such as the local conservative property and the robustness with the unstructured meshes and so on. In generally, two different function spaces are used in the finite volume element method, so the theory and numerical analysis of it are more difficult than that of the finite difference method and the finite element method.

Up to now, the basic theory of finite volume element method has reached a relatively perfect point, and there are many references in this field. Bank and Rose compared the finite element method with the finite volume element method in Cai [Cai (1990)]. In Ewing et al. [Ewing, Lin and Lin (2002)], the authors obtained the error estimation of the maximum norm in the finite volume element method. The finite volume element method was used to solve the diffusion equation problem, and the error analysis was given in Cai et al. [Cai and McCormick (1990)]. The authors in Plexousakis et al. [Plexousakis and Zouraris (2004)] used a class of high-order finite volume element methods to solve one-dimensional elliptical equations. In Chen et al. [Chen, Wu and Xu (2012)], Chen studied the higher-order finite volume element method more deeply. Professor Chen and her students solved the elliptical and parabolic optimal control problems by using the finite volume element method and gave the corresponding error estimates in Luo et al. [Luo, Chen, Huang et al. (2014); Luo, Chen and Huang (2013)]. Chatzipantelidis et al. [Chatzipantelidis, Lazarov and Thomée (2004)] used the finite volume element method to solve the parabolic optimal control problem in convex polygons and give the corresponding error estimates. In Wang et al. [Wang and Zhang (2019)], the authors proposed a stabilized immersed finite volume element method for solving elliptic interface problems on Cartesian mesh. Furthermore, other results of finite volume element method can be seen in Bank et al. [Bank and Rose (1987); Chen (2010); Li, Li, He et al. (2018); Luo (2014); Zhao, Chen, Gao et al. (2013)].

Alternating direction implicit methods have proven valuable in the approximation of the solutions of parabolic and hyperbolic problems. This technique was first introduced by Douglas [Douglas (1955)] in 1955 to solve a multidimensional parabolic problem by treating it as a sequence of one-dimensional problems. Since then, several closely related methods have been introduced for solving parabolic and hyperbolic problems. In Zhang et al. [Zhang and Deng (2007)], a new alternating-direction finite element method was presented for solving hyperbolic equation. A new matched alternating direction implicit method is proposed in Wei et al. [Wei, Li and Zhao (2018)] for solving three-dimensional parabolic interface problems with discontinuous jumps and complex interfaces. An ADI quadratic finite volume element method was given for solving second order hyperbolic problems in Yang et al. [Yang and Chen (2009)]. Samir Karaa did a lot of research about this field [Karaa (2009, 2010b); Karaa and Zhang (2004)]. In Karaa [Karaa (2006)], he derived a high-order compact alternating direction implicit method for solving three-dimensional unsteady convection-diffusion problems and obtained the order in space and in time are fourth and second, respectively. In Ge et al. [Ge, Tian and Zhang (2013)], the authors developed an exponential high order compact alternating direction implicit method for solving three dimensional unsteady convection diffusion equations and compared it with the method of Karaa [Karaa (2006)]. In addition, ADI also played an important role in other areas. For instance, a backward Euler alternating direction implicit (ADI) difference scheme was formulated and analyzed for the three-dimensional fractional evolution equation in Chen et al. [Chen, Xu, Cao et al. (2018)]. An ADI difference scheme based on fractional trapezoidal rule was proposed to solve fractional integro-differential equation with a weakly singular kernel in Qiao et al. [Qiao, Xu and Wang (2019)]. In Zhou et al. [Zhou and Xu (2019)], the authors presented an alternating direction implicit (ADI) difference scheme for the multi-term time-fractional integro-differential equation with a weakly singular kernel. An alternating direction implicit spectral method is developed to solve the initial boundary value problem of the two-dimensional multi-term time fractional mixed diffusion and diffusion-wave equations in Liu et al. [Liu, Liu and Zeng (2019)]. The system of 2-D Burgers equations is numerically solved by using alternating direction implicit method in Celikten et al.

[Celikten and Aksan (2019)]. For more relevant literature, we can refer to Li et al. [Li, Liao and Lin (2019); Zhang and Wang (2004); Gao and Sun (2016); Vong and Wang (2015); Chen (2012); Wang and Zhao (2003); Wang (2008); Koutserimpas, Papadopoulos and Glytsis (2017); Qiao and Xu (2018); Zhao (2015).]

In this article, we combine finite volume element methods and alternating direction implicit methods for solving Eq. (1). The goal of this paper is to extend the method to the class of equations represented by Eq. (1) and improve the computational efficiency of the finite volume element method. An outline of the paper is as follows: In Section 2, we derive the ADI finite volume element schemes in tensor product form. Using the Douglas alternating direction discrete method, we successfully convert a multidimensional problem to a series of one- dimensional problems, which can be solved very easily. In Section 3, we further analyze the scheme and obtain optimal L^2 norm error estimate. Section 4 provides four numerical experiments to illustrate the effectiveness of the scheme. Our schemes compare well with other schemes. Section 5 gives some conclusions.

1.1 Fully-discrete ADI finite volume element scheme

In this section, we consider the two-dimensional problem on a domain $\Omega=[0,1]\times[0,1]$.

In order to solve problem Eq. (1), let $v=u_t+\gamma_1 u$, then Eq. (1) can be rewritten as

$$
\begin{aligned}
&(a) \quad v_t - \nabla\cdot(Q\nabla v) + \nabla\cdot(\gamma_1 Q - A)\nabla u = S(x,y,t), (x,y)\in\Omega, t>0,\\
&(b) \quad v = u_t + \gamma_1 u, (x,y)\in\Omega, t>0,\\
&(c) \quad u=0, v=0, (x,y)\in\partial\Omega, t>0,\\
&(d) \quad u(x,y,0)=u_0(x,y), v(x,y,0)=u_1(x,y)+\gamma_1 u_0(x,y), (x,y)\in\Omega.
\end{aligned}
\tag{2}
$$

In order to get the solution of Eq. (2), we consider a rectangular partition Q_h for the domain Ω and denote by (x_i,y_j), (i=0,1,…,N_x, j=0,1,…,N_y). Let $h_i^x=x_i-x_{i-1}$, (i=1,2,…,N_x), $h_j^y=y_j-y_{j-1}$, (j=1,2,…,N_y), $h^x=\max\limits_{1\le i\le N_x} h_i^x$, $h^y=\max\limits_{1\le j\le N_y} h_j^y$, $h=\max(h^x,h^y)$. Further let $x_{i-\frac12}=x_i-\frac12 h_i^x$, ($i$=1,2,…,$N_x$), $y_{j-\frac12}=y_j-\frac12 h_j^y$, ($j$=1,2,…,$N_y$), $h^x_{i+\frac12}=x_{i+\frac12}-x_{i-\frac12}$, ($i$=1,2,…, N_x−1), $h^y_{j+\frac12}=y_{j+\frac12}-y_{j-\frac12}$, ($j$=1,2,…, N_y−1). Then $\Omega_{ij}^*=[x_{i-\frac12},x_{i+\frac12}]\times[y_{j-\frac12},y_{j+\frac12}]$ is a control volume or dual element of (x_i,y_j). All control volumes constitute the dual partition Q_h^* of domain ω. Let $\delta\ t$ denote the time step size, and $t^n=n\Delta t$ (n=0,1,…), $t^{n-\frac12}=t^n-\dfrac{\Delta t}{2}$ (n=1,2,…), $u^n=u^n(t_n)$. At time $t=t^{n-\frac12}$, using the *Crank − Nicolson* scheme (or *central difference*), we obtain the differential scheme of Eqs. (2*a*) and (2*b*) respectively:

$$\frac{v^n - v^{n-1}}{\Delta t} - \nabla \cdot (Q\nabla \frac{v^n + v^{n-1}}{2}) + \nabla \cdot (\gamma_1 Q - A)\nabla \frac{u^n + u^{n-1}}{2} = \frac{1}{\Delta t}\int_{t^{n-1}}^{t^n} Sdt + R_1^{n-\frac{1}{2}}, \tag{3}$$

$$\frac{u^n - u^{n-1}}{\Delta t} = \frac{v^n + v^{n-1}}{2} - \gamma_1 \frac{u^n + u^{n-1}}{2} + R_2^{n-\frac{1}{2}}, \tag{4}$$

where

$$\begin{aligned} R_1^{n-\frac{1}{2}} = & \frac{1}{2\Delta t}\int_{t^{n-1}}^{t^n} \nabla \cdot Q\nabla v_{tt}(\theta_3(t))(t-t^n)(t-t^{n-1})dt \\ & + \frac{1}{2\Delta t}\int_{t^{n-1}}^{t^n} \nabla \cdot (A - \gamma_1 Q)\nabla v_{tt}(\theta_3(t))(t-t^n)(t-t^{n-1})dt, \end{aligned}$$

$$\begin{aligned} R_2^{n-\frac{1}{2}} = & \frac{1}{2\Delta t}\int_{t^{n-1}}^{t^n} \frac{\partial^2 v}{\partial t^2}(\theta_1(t))(t-t^n)(t-t^{n-1})dt \\ & - \frac{\gamma_1}{2\Delta t}\int_{t^{n-1}}^{t^n} \frac{\partial^2 u}{\partial t^2}(\theta_2(t))(t-t^n)(t-t^{n-1})dt. \end{aligned}$$

From Eq. (4), we can express u^n as

$$u^n = \frac{\Delta t}{2 + \gamma_1 \Delta t}(v^n + v^{n-1}) + \frac{2 - \gamma_1 \Delta t}{2 + \gamma_1 \Delta t}u^{n-1} + \frac{2\Delta t}{2 + \gamma_1 \Delta t}R_2^{n-\frac{1}{2}}. \tag{5}$$

Substituting Eq. (5) into Eq. (3) results in

$$\begin{aligned} \frac{v^n - v^{n-1}}{\Delta t} - \nabla \cdot (G\nabla \frac{v^n + v^{n-1}}{2}) + \nabla \cdot (H\nabla u^{n-1}) \\ = \frac{1}{\Delta t}\int_{t^{n-1}}^{t^n} Sdt + R_1^{n-\frac{1}{2}} + \frac{\Delta t}{2 + \gamma_1 \Delta t}\nabla \cdot (A - \gamma_1 Q)\nabla R_2^{n-\frac{1}{2}}, \end{aligned} \tag{6}$$

where

$$G = \frac{2}{2 + \gamma_1 \Delta t}Q + \frac{\Delta t}{2 + \gamma_1 \Delta t}A = diag(g_1, g_2),$$

$$H = \frac{2\gamma_1}{2 + \gamma_1 \Delta t}Q - \frac{2}{2 + \gamma_1 \Delta t}A = diag(h_1, h_2).$$

Denote $U = H_0^1(\Omega) \cap H^2(\Omega)$. Integrate Eq. (6) over Ω_{ij}^*, then using Green formula, the conservative integral form of Eq. (6) reads: Finding $u^n \in U$, such that

$$\int\int_{\Omega_{ij}^*} \frac{v^n - v^{n-1}}{\Delta t} dxdy - \left[\int_{\partial\Omega_{ij}^*} g_1(\frac{v^n + v^{n-1}}{2})_x dy - g_2(\frac{v^n + v^{n-1}}{2})_y dx \right] + \int_{\partial\Omega_{ij}^*} h_1 u_x^{n-1} dy - h_2 u_y^{n-1} dx = \frac{1}{\Delta t} \int\int_{\Omega_{ij}^*} \int_{t^{n-1}}^{t^n} S dt dx dy + R_{12}^{n-\frac{1}{2}}, \tag{7}$$

where $i = 1, 2, \ldots, j = 1, 2, \ldots,$

$$R_{12}^{n-\frac{1}{2}} = \int_{\Omega_{ij}^*} \left[R_1^{n-\frac{1}{2}} + \frac{\Delta t}{2 + \gamma_1 \Delta t} \nabla \cdot (A - \gamma_1 Q) \nabla R_2^{n-\frac{1}{2}} \right] dxdy.$$

Suppose U_h is a trial function space over the partition Q_h, which is obtained by bilinear interpolation. Let $\pi\ u^n$ and $\pi\ v^n$ be the interpolation function of u^n and v^n onto the the trial function space U_h, respectively. Then, in Eq. (4) and Eq. (7), respectively, we get

$$\frac{\pi u^n - \pi u^{n-1}}{\Delta t} = \frac{\pi v^n + \pi v^{n-1}}{2} - \gamma_1 \frac{\pi u^n + \pi u^{n-1}}{2} + R_3^{n-\frac{1}{2}}, \tag{8}$$

$$\int\int_{\Omega_{ij}^*} \frac{\pi v^n - \pi v^{n-1}}{\Delta t} dxdy - \left[\int_{\partial\Omega_{ij}^*} g_1(\frac{\pi v^n + \pi v^{n-1}}{2})_x dy - g_2(\frac{\pi v^n + \pi v^{n-1}}{2})_y dx \right] + \int_{\partial\Omega_{ij}^*} h_1 \pi u_x^{n-1} dy - h_2 \pi u_y^{n-1} dx = \frac{1}{\Delta t} \int\int_{\Omega_{ij}^*} \int_{t^{n-1}}^{t^n} S dt dx dy + R_{12}^{n-\frac{1}{2}} + R_4^{n-\frac{1}{2}}, \tag{9}$$

where

$$R_3^{n-\frac{1}{2}} = \frac{(\pi u^n - u^n) - (\pi u^{n-1} - u^{n-1})}{\Delta t} + \gamma_1 \frac{(\pi u^n + u^n) + (\pi u^{n-1} + u^{n-1})}{2} - \frac{(\pi v^n - v^n) + (\pi v^{n-1} - v^{n-1})}{2},$$

$$
\begin{aligned}
R_4^{n-\frac{1}{2}} = & \int\int_{\Omega_{ij}^*} \frac{\pi v^n - \pi v^{n-1}}{\Delta t} dxdy - \int\int_{\Omega_{ij}^*} \frac{v^n - v^{n-1}}{\Delta t} dxdy \\
& - \left[\int_{\partial\Omega_{ij}^*} g_1 (\frac{\pi v^n + \pi v^{n-1}}{2})_x dy - g_2 (\frac{\pi v^n + \pi v^{n-1}}{2})_y dx \right] \\
& + \left[\int_{\partial\Omega_{ij}^*} g_1 (\frac{v^n + v^{n-1}}{2})_x dy - g_2 (\frac{v^n + v^{n-1}}{2})_y dx \right] \\
& + \int_{\partial\Omega_{ij}^*} h_1 \pi u_x^{n-1} dy - h_2 \pi u_y^{n-1} dx - \int_{\partial\Omega_{ij}^*} h_1 u_x^{n-1} dy - h_2 u_y^{n-1} dx.
\end{aligned}
$$

Assume $\{\alpha_k(x)\}$ $(k = 0, 1, \cdots, N_x)$, $\{\beta_l(y)\}(l = 0, 1, \cdots, N_y)$, are the linear interpolating basis functions in x and y directions respectively.

$$
\alpha_k(x) = \begin{cases} 1 - \frac{1}{h_k^x}, & x_{k-1} \le x \le x_k; \\ 1 - \frac{1}{h_{k+1}^x}, & x_k \le x \le x_{k+1}; \\ 0, & \text{elsewhere}; \end{cases} \qquad \beta_l(y) = \begin{cases} 1 - \frac{1}{h_l^y}, & y_{l-1} \le y \le y_l; \\ 1 - \frac{1}{h_{l+1}^y}, & y_l \le y \le y_{l+1}; \\ 0, & \text{elsewhere}. \end{cases}
$$

Then $\{\alpha_k(x)\beta_l(y)\}$ are basis functions of U_h. That is, for $u_h^n, v_h^n \in U_h$, we have

$$
u_h^n = \sum_{k=0}^{N_x} \sum_{l=0}^{N_y} u_{kl}^n \alpha_k(x) \beta_l(y), \qquad v_h^n = \sum_{k=0}^{N_x} \sum_{l=0}^{N_y} v_{kl}^n \alpha_k(x) \beta_l(y),
$$

where $u_{kl}^n = u_h^n(x_k, y_l)$ and $v_{kl}^n = v_h^n(x_k, y_l)$.

Dropping the error terms, substituting πu^n, πv^n by $u_h^n, v_h^n \in U_h$ in Eq. (8) and Eq. (9), we obtain the finite volume element scheme corresponding to Eqs. (2a) and (2b)

$$
\begin{aligned}
& \int\int_{\Omega_{ij}^*} \frac{v_h^n - v_h^{n-1}}{\Delta t} dxdy - \left[\int_{\partial\Omega_{ij}^*} g_1 (\frac{v_h^n + v_h^{n-1}}{2})_x dy - g_2 (\frac{v_h^n + v_h^{n-1}}{2})_y dx \right] \\
& \qquad + \int_{\partial\Omega_{ij}^*} h_1 (u_h^{n-1})_x dy - h_2 (u_h^{n-1})_y dx = \frac{1}{\Delta t} \int\int_{\Omega_{ij}^*} \int_{t^{n-1}}^{t^n} S dt dx dy,
\end{aligned} \tag{10}
$$

$$
\frac{u_h^n - u_h^{n-1}}{\Delta t} = \frac{v_h^n + v_h^{n-1}}{2} - \gamma_1 \frac{u_h^n + u_h^{n-1}}{2}. \tag{11}
$$

Dealing with variable coefficients, we denote

$$\bar{g}_1(x_{i-\frac{1}{2}},y_j)=\frac{1}{h^y_{j+\frac{1}{2}}}\int_{y_{j-\frac{1}{2}}}^{y_{j+\frac{1}{2}}}g_1(x_{i-\frac{1}{2}},y)dy,\qquad \bar{g}_1(x_{i+\frac{1}{2}},y_j)=\frac{1}{h^y_{j+\frac{1}{2}}}\int_{y_{j-\frac{1}{2}}}^{y_{j+\frac{1}{2}}}g_1(x_{i+\frac{1}{2}},y)dy,$$

$$\bar{g}_2(x_i,y_{j-\frac{1}{2}})=\frac{1}{h^x_{i+\frac{1}{2}}}\int_{x_{i-\frac{1}{2}}}^{x_{i+\frac{1}{2}}}g_2(x,y_{j-\frac{1}{2}})dx,\qquad \bar{g}_2(x_i,y_{j+\frac{1}{2}})=\frac{1}{h^x_{i+\frac{1}{2}}}\int_{x_{i-\frac{1}{2}}}^{x_{i+\frac{1}{2}}}g_2(x,y_{j+\frac{1}{2}})dx,$$

$$\bar{h}_1(x_{i-\frac{1}{2}},y_j)=\frac{1}{h^y_{j+\frac{1}{2}}}\int_{y_{j-\frac{1}{2}}}^{y_{j+\frac{1}{2}}}h_1(x_{i-\frac{1}{2}},y)dy,\qquad \bar{h}_1(x_{i+\frac{1}{2}},y_j)=\frac{1}{h^y_{j+\frac{1}{2}}}\int_{y_{j-\frac{1}{2}}}^{y_{j+\frac{1}{2}}}h_1(x_{i+\frac{1}{2}},y)dy,$$

$$\bar{h}_2(x_i,y_{j-\frac{1}{2}})=\frac{1}{h^x_{i+\frac{1}{2}}}\int_{x_{i-\frac{1}{2}}}^{x_{i+\frac{1}{2}}}h_2(x,y_{j-\frac{1}{2}})dx,\qquad \bar{h}_2(x_i,y_{j+\frac{1}{2}})=\frac{1}{h^x_{i+\frac{1}{2}}}\int_{x_{i-\frac{1}{2}}}^{x_{i+\frac{1}{2}}}h_2(x,y_{j+\frac{1}{2}})dx.$$

In Eq. (10), we can obtain

$$\begin{aligned}\int\int_{\Omega^*_{ij}}\frac{v_h^n-v_h^{n-1}}{\Delta t}dxdy-\Bigg[&-\bar{g}_2(x_i,y_{j-\frac{1}{2}})\int_{x_{i-\frac{1}{2}}}^{x_{i+\frac{1}{2}}}\Big(\frac{v_h^n+v_h^{n-1}}{2}\Big)_y(x,y_{j-\frac{1}{2}})dx\\
&+\bar{g}_2(x_i,y_{j+\frac{1}{2}})\int_{x_{i-\frac{1}{2}}}^{x_{i+\frac{1}{2}}}\Big(\frac{v_h^n+v_h^{n-1}}{2}\Big)_y(x,y_{j+\frac{1}{2}})dx\\
&+\bar{g}_1(x_{i+\frac{1}{2}},y_j)\int_{y_{i-\frac{1}{2}}}^{y_{i+\frac{1}{2}}}\Big(\frac{v_h^n+v_h^{n-1}}{2}\Big)_x(x_{i+\frac{1}{2}},y)dy\\
&-\bar{g}_1(x_{i-\frac{1}{2}},y_j)\int_{y_{i-\frac{1}{2}}}^{y_{i+\frac{1}{2}}}\Big(\frac{v_h^n+v_h^{n-1}}{2}\Big)_x(x_{i-\frac{1}{2}},y)dy\Bigg]\\
+\Bigg[&-\bar{h}_2(x_i,y_{j-\frac{1}{2}})\int_{x_{i-\frac{1}{2}}}^{x_{i+\frac{1}{2}}}(u_h^{n-1})_y(x,y_{j-\frac{1}{2}})dx\\
&+\bar{h}_2(x_i,y_{j+\frac{1}{2}})\int_{x_{i-\frac{1}{2}}}^{x_{i+\frac{1}{2}}}(u_h^{n-1})_y(x,y_{j+\frac{1}{2}})dx\\
&+\bar{h}_1(x_{i+\frac{1}{2}},y_j)\int_{y_{i-\frac{1}{2}}}^{y_{i+\frac{1}{2}}}(u_h^{n-1})_x(x_{i+\frac{1}{2}},y)dy\\
&-\bar{h}_1(x_{i-\frac{1}{2}},y_j)\int_{y_{i-\frac{1}{2}}}^{y_{i+\frac{1}{2}}}(u_h^{n-1})_x(x_{i-\frac{1}{2}},y)dy\Bigg]\\
&=\frac{1}{\Delta t}\int\int_{\Omega^*_{ij}}\int_{t^{n-1}}^{t^n}Sdtdxdy.\end{aligned}\tag{12}$$

Let

$$
\begin{aligned}
U^n &= \left[u_{11}^n, u_{12}^n, \cdots, u_{1N_y-1}^n, u_{21}^n, u_{22}^n, \cdots, u_{2N_y-1}^n, \cdots, u_{N_x-11}^n, \cdots, u_{N_x-1N_y-1}^n\right]^T,\\
V^n &= \left[v_{11}^n, v_{12}^n, \cdots, v_{1N_y-1}^n, v_{21}^n, v_{22}^n, \cdots, v_{2N_y-1}^n, \cdots, v_{N_x-11}^n, \cdots, v_{N_x-1N_y-1}^n\right]^T,\\
C_x &= \left[\int_{x_{i-\frac{1}{2}}}^{x_{i+\frac{1}{2}}} \alpha_k(x)dx\right]_{(N_x-1)\times(N_y-1)},\\
C_y &= \left[\int_{y_{j-\frac{1}{2}}}^{y_{j+\frac{1}{2}}} \beta_l(y)dy\right]_{(N_x-1)\times(N_y-1)},\\
A_x &= \left[\bar{g}_1(x_{i-\frac{1}{2}}, y_j)\alpha_k'(x_{i-\frac{1}{2}}) - \bar{g}_1(x_{i+\frac{1}{2}}, y_j)\alpha_k'(x_{i+\frac{1}{2}})\right]_{(N_x-1)\times(N_y-1)},\\
A_y &= \left[\bar{g}_2(x_i, y_{j-\frac{1}{2}})\beta_l'(y_{j-\frac{1}{2}}) - \bar{g}_2(x_i, y_{j+\frac{1}{2}})\beta_l'(y_{j+\frac{1}{2}})\right]_{(N_x-1)\times(N_y-1)},\\
B_x &= \left[\bar{h}_1(x_{i-\frac{1}{2}}, y_j)\alpha_k'(x_{i-\frac{1}{2}}) - \bar{h}_1(x_{i+\frac{1}{2}}, y_j)\alpha_k'(x_{i+\frac{1}{2}})\right]_{(N_x-1)\times(N_y-1)},\\
B_y &= \left[\bar{h}_2(x_i, y_{j-\frac{1}{2}})\beta_l'(y_{j-\frac{1}{2}}) - \bar{h}_2(x_i, y_{j+\frac{1}{2}})\beta_l'(y_{j+\frac{1}{2}})\right]_{(N_x-1)\times(N_y-1)},\\
\Phi^n &= \left[\frac{1}{\Delta t}\int\int_{\Omega_{ij}^*}\int_{t^{n-1}}^{t^n} S dt dx dy\right]_{(N_x-1)(N_y-1)}^T.
\end{aligned}
$$

Using the above notations, Eq. (11) and Eq. (12) can be written as the following tensor product form

$$
\begin{aligned}
C_x \otimes C_y(V^n - V^{n-1}) + \frac{\Delta t}{2}(C_x \otimes A_y + A_x \otimes C_y)(V^n + V^{n-1})\\
= \Delta t \Phi^n + \Delta t(C_x \otimes B_y + B_x \otimes C_y)U^{n-1},
\end{aligned}
\tag{13}
$$

$$
U^n = \frac{\Delta t}{2 + \gamma_1 \Delta t}(V^n + V^{n-1}) + \frac{2 - \gamma_1 \Delta t}{2 + \gamma_1 \Delta t}U^{n-1},
\tag{14}
$$

where $\otimes$ represents Kronecker tensor product. Eqs. (13) and (14) are fully discrete finite volume element schemes of Eqs. (2a) and (2b).

Adding a perturbation term

$$
\frac{(\Delta t)^2}{4}A_x \otimes A_y(V^n - V^{n-1})
$$

to Eq. (13), then

$$
\begin{aligned}
C_x \otimes C_y(V^n - V^{n-1}) + \frac{\Delta t}{2}(C_x \otimes A_y + A_x \otimes C_y)(V^n + V^{n-1})\\
+ \frac{(\Delta t)^2}{4}A_x \otimes A_y(V^n - V^{n-1}) = \Delta t \Phi^n + \Delta t(C_x \otimes B_y + B_x \otimes C_y)U^{n-1}.
\end{aligned}
\tag{15}
$$

Eq. (15) can be rewritten as

$$\begin{aligned}(C_x\otimes I+\frac{\Delta t}{2}A_x\otimes I)(I\otimes C_y+\frac{\Delta t}{2}I\otimes A_y)V^n=(C_x\otimes I\\ -\frac{\Delta t}{2}A_x\otimes I)(I\otimes C_y-\frac{\Delta t}{2}I\otimes A_y)V^{n-1}+\Delta t\Phi^n+\Delta t(C_x\otimes B_y+B_x\otimes C_y)U^{n-1}.\end{aligned}\tag{16}$$

Using the Douglas alternating direction discrete method, two sides of the Eq. (16) minus

$$(C_x\otimes I+\frac{\Delta t}{2}A_x\otimes I)(I\otimes C_y+\frac{\Delta t}{2}I\otimes A_y)V^{n-1},$$

we can obtain

$$\begin{aligned}&(C_x\otimes I+\frac{\Delta t}{2}A_x\otimes I)(I\otimes C_y+\frac{\Delta t}{2}I\otimes A_y)(V^n-V^{n-1})\\ &=-\Delta t(C_x\otimes A_y+A_x\otimes C_y)V^{n-1}+\Delta t\Phi^n+\Delta t(C_x\otimes B_y+B_x\otimes C_y)U^{n-1}.\end{aligned}\tag{17}$$

In practical computation, design the following calculation steps:

Step 1: Compute initial vectors U^0 and V^0 by the initial conditions Eq. (2d);

Step 2: Compute $V^{\frac{n-1}{2}}-V^{n-1}$ by

$$\begin{aligned}(C_x\otimes I+\frac{\Delta t}{2}A_x\otimes I)(V^{n-\frac{1}{2}}-V^{n-1})=&\Delta t\Phi^n-\Delta t(C_x\otimes A_y+A_x\otimes C_y)V^{n-1}\\ &+\Delta t(C_x\otimes B_y+B_x\otimes C_y)U^{n-1}\end{aligned}$$

Step 3: Compute V^n-V^{n-1}

$$(I\otimes C_y+\frac{\Delta t}{2}I\otimes A_y)(V^n-V^{n-1})=V^{n-\frac{1}{2}}-V^{n-1};$$

Step 4: Compute V^n as

$$V^n=(V^n-V^{n-1})+V^{n-1};$$

Step 5: Substitute V^n in Eq. (14), and we can obtain U^n.

1.2 Error estimates

We have derived the ADI finite volume element schemes in Section 2. In this section, we further analyze the convergence of these schemes with respect to the L^2 norm. Let $\xi=\pi u-u_h,\eta=\pi v-v_h$. From Eqs. (8), (9), (11) and (15), we can obtain the error estimate equations

$$\frac{\xi^n-\xi^{n-1}}{\Delta t}=\frac{\eta^n+\eta^{n-1}}{2}-\gamma_1\frac{\xi^n+\xi^{n-1}}{2}+R_2^{n-\frac{1}{2}}+R_3^{n-\frac{1}{2}},\tag{18}$$

$$
\begin{aligned}
\int\int_{\Omega_{ij}^*}\frac{\eta^n-\eta^{n-1}}{\Delta t}dxdy-\Bigg[&-\bar{q}_2(x_i,y_{j-\frac{1}{2}})\int_{x_{i-\frac{1}{2}}}^{x_{i+\frac{1}{2}}}(\frac{\eta^n+\eta^{n-1}}{2})_y(x,y_{j-\frac{1}{2}})dx\\
&+\bar{q}_2(x_i,y_{j+\frac{1}{2}})\int_{x_{i-\frac{1}{2}}}^{x_{i+\frac{1}{2}}}(\frac{\eta^n+\eta^{n-1}}{2})_y(x,y_{j+\frac{1}{2}})dx\\
&+\bar{q}_1(x_{i+\frac{1}{2}},y_j)\int_{y_{i-\frac{1}{2}}}^{y_{i+\frac{1}{2}}}(\frac{\eta^n+\eta^{n-1}}{2})_x(x_{i+\frac{1}{2}},y)dy\\
&-\bar{q}_1(x_{i-\frac{1}{2}},y_j)\int_{y_{i-\frac{1}{2}}}^{y_{i+\frac{1}{2}}}(\frac{\eta^n+\eta^{n-1}}{2})_x(x_{i-\frac{1}{2}},y)dy\Bigg]\\
+\frac{\Delta t}{4}\Bigg[&\bar{g}_1(x_{i+\frac{1}{2}},y_j)\bar{g}_2(x_i,y_{j+\frac{1}{2}})\frac{\partial^2(\eta^n-\eta^{n-1})}{\partial x\partial y}(x_{i+\frac{1}{2}},y_{j+\frac{1}{2}})\\
&-\bar{g}_1(x_{i+\frac{1}{2}},y_j)\bar{g}_2(x_i,y_{j-\frac{1}{2}})\frac{\partial^2(\eta^n-\eta^{n-1})}{\partial x\partial y}(x_{i+\frac{1}{2}},y_{j-\frac{1}{2}})\\
&-\bar{g}_1(x_{i-\frac{1}{2}},y_j)\bar{g}_2(x_i,y_{j+\frac{1}{2}})\frac{\partial^2(\eta^n-\eta^{n-1})}{\partial x\partial y}(x_{i-\frac{1}{2}},y_{j+\frac{1}{2}})\\
&+\bar{g}_1(x_{i-\frac{1}{2}},y_j)\bar{g}_2(x_i,y_{j-\frac{1}{2}})\frac{\partial^2(\eta^n-\eta^{n-1})}{\partial x\partial y}(x_{i-\frac{1}{2}},y_{j-\frac{1}{2}})\Bigg]\\
+\Bigg[&-\bar{h}_2(x_i,y_{j-\frac{1}{2}})\int_{x_{i-\frac{1}{2}}}^{x_{i+\frac{1}{2}}}(\xi^{n-1})_y(x,y_{j-\frac{1}{2}})dx\\
&+\bar{h}_2(x_i,y_{j+\frac{1}{2}})\int_{x_{i-\frac{1}{2}}}^{x_{i+\frac{1}{2}}}(\xi^{n-1})_y(x,y_{j+\frac{1}{2}})dx\\
&+\bar{h}_1(x_{i+\frac{1}{2}},y_j)\int_{y_{i-\frac{1}{2}}}^{y_{i+\frac{1}{2}}}(\xi^{n-1})_x(x_{i+\frac{1}{2}},y)dy\\
&-\bar{h}_1(x_{i-\frac{1}{2}},y_j)\int_{y_{i-\frac{1}{2}}}^{y_{i+\frac{1}{2}}}(\xi^{n-1})_x(x_{i-\frac{1}{2}},y)dy\Bigg]\\
&=R_{12}^{n-\frac{1}{2}}+R_4^{n-\frac{1}{2}}+R_5^{n-\frac{1}{2}}+R_6^{n-\frac{1}{2}},
\end{aligned}
\tag{19}
$$

where

$$
\begin{aligned}
R_5^{n-\frac{1}{2}} = & \Bigg[-\int_{x_{i-\frac{1}{2}}}^{x_{i+\frac{1}{2}}} (g_2(x, y_{j-\frac{1}{2}}) - \bar{g}_2(x_i, y_{j-\frac{1}{2}}))(\frac{\pi v^n + \pi v^{n-1}}{2})_y(x, y_{j-\frac{1}{2}})dx \\
& + \int_{x_{i-\frac{1}{2}}}^{x_{i+\frac{1}{2}}} (g_2(x, y_{j+\frac{1}{2}}) - \bar{g}_2(x_i, y_{j+\frac{1}{2}}))(\frac{\pi v^n + \pi v^{n-1}}{2})_y(x, y_{j+\frac{1}{2}})dx \\
& + \int_{y_{i-\frac{1}{2}}}^{y_{i+\frac{1}{2}}} (g_1(x_{i+\frac{1}{2}}, y) - \bar{g}_1(x_{i+\frac{1}{2}}, y_j))(\frac{\pi v^n + \pi v^{n-1}}{2})_x(x_{i+\frac{1}{2}}, y)dy \\
& - \int_{y_{i-\frac{1}{2}}}^{y_{i+\frac{1}{2}}} (g_1(x_{i-\frac{1}{2}}, y) - \bar{g}_1(x_{i-\frac{1}{2}}, y_j))(\frac{\pi v^n + \pi v^{n-1}}{2})_x(x_{i-\frac{1}{2}}, y)dy \Bigg] \\
& - \Bigg[-\int_{x_{i-\frac{1}{2}}}^{x_{i+\frac{1}{2}}} (h_2(x, y_{j-\frac{1}{2}}) - \bar{h}_2(x_i, y_{j-\frac{1}{2}}))(\pi u^{n-1})_y(x, y_{j-\frac{1}{2}})dx \\
& + \int_{x_{i-\frac{1}{2}}}^{x_{i+\frac{1}{2}}} (h_2(x, y_{j+\frac{1}{2}}) - \bar{h}_2(x_i, y_{j+\frac{1}{2}}))(\pi u^{n-1})_y(x, y_{j+\frac{1}{2}})dx \\
& + \int_{y_{i-\frac{1}{2}}}^{y_{i+\frac{1}{2}}} (h_1(x_{i+\frac{1}{2}}, y) - \bar{h}_1(x_{i+\frac{1}{2}}, y_j))(\pi u^{n-1})_x(x_{i+\frac{1}{2}}, y)dy \\
& - \int_{y_{i-\frac{1}{2}}}^{y_{i+\frac{1}{2}}} (h_1(x_{i-\frac{1}{2}}, y)\bar{h}_1(x_{i-\frac{1}{2}}, y_j))(\pi u^{n-1})_x(x_{i-\frac{1}{2}}, y)dy \Bigg],
\end{aligned}
$$

$$
\begin{aligned}
R_6^{n-\frac{1}{2}} = & \frac{\Delta t}{4} \Bigg[\bar{g}_1(x_{i+\frac{1}{2}}, y_j)\bar{g}_2(x_i, y_{j+\frac{1}{2}}) \frac{\partial^2(\pi v^n - \pi v^{n-1})}{\partial x \partial y}(x_{i+\frac{1}{2}}, y_{j+\frac{1}{2}}) \\
& - \bar{g}_1(x_{i+\frac{1}{2}}, y_j)\bar{g}_2(x_i, y_{j-\frac{1}{2}}) \frac{\partial^2(\pi v^n - \pi v^{n-1})}{\partial x \partial y}(x_{i+\frac{1}{2}}, y_{j-\frac{1}{2}}) \\
& - \bar{g}_1(x_{i-\frac{1}{2}}, y_j)\bar{g}_2(x_i, y_{j+\frac{1}{2}}) \frac{\partial^2(\pi v^n - \pi v^{n-1})}{\partial x \partial y}(x_{i-\frac{1}{2}}, y_{j+\frac{1}{2}}) \\
& + \bar{g}_1(x_{i-\frac{1}{2}}, y_j)\bar{g}_2(x_i, y_{j-\frac{1}{2}}) \frac{\partial^2(\pi v^n - \pi v^{n-1})}{\partial x \partial y}(x_{i-\frac{1}{2}}, y_{j-\frac{1}{2}}) \Bigg].
\end{aligned}
$$

Let $K = A - \gamma_1 Q = diag\{k_1, k_2\}$. Collecting Eqs. (18) and (19), we obtain

$$
\begin{aligned}
\int\int_{\Omega_{ij}^*} \frac{\eta^n - \eta^{n-1}}{\Delta t} dxdy - \Bigg[& -\bar{q}_2(x_i, y_{j-\frac{1}{2}}) \int_{x_{i-\frac{1}{2}}}^{x_{i+\frac{1}{2}}} (\frac{\eta^n + \eta^{n-1}}{2})_y (x, y_{j-\frac{1}{2}}) dx \\
& + \bar{q}_2(x_i, y_{j+\frac{1}{2}}) \int_{x_{i-\frac{1}{2}}}^{x_{i+\frac{1}{2}}} (\frac{\eta^n + \eta^{n-1}}{2})_y (x, y_{j+\frac{1}{2}}) dx \\
& + \bar{q}_1(x_{i+\frac{1}{2}}, y_j) \int_{y_{i-\frac{1}{2}}}^{y_{i+\frac{1}{2}}} (\frac{\eta^n + \eta^{n-1}}{2})_x (x_{i+\frac{1}{2}}, y) dy \\
& - \bar{q}_1(x_{i-\frac{1}{2}}, y_j) \int_{y_{i-\frac{1}{2}}}^{y_{i+\frac{1}{2}}} (\frac{\eta^n + \eta^{n-1}}{2})_x (x_{i-\frac{1}{2}}, y) dy \Bigg] \\
& - \Bigg[-\bar{k}_2(x_i, y_{j-\frac{1}{2}}) \int_{x_{i-\frac{1}{2}}}^{x_{i+\frac{1}{2}}} (\frac{\xi^n + \xi^{n-1}}{2})_y (x, y_{j-\frac{1}{2}}) dx \\
& + \bar{k}_2(x_i, y_{j+\frac{1}{2}}) \int_{x_{i-\frac{1}{2}}}^{x_{i+\frac{1}{2}}} (\frac{\xi^n + \xi^{n-1}}{2})_y (x, y_{j+\frac{1}{2}}) dx \\
& + \bar{k}_1(x_{i+\frac{1}{2}}, y_j) \int_{y_{i-\frac{1}{2}}}^{y_{i+\frac{1}{2}}} (\frac{\xi^n + \xi^{n-1}}{2})_x (x_{i+\frac{1}{2}}, y) dy \\
& - \bar{k}_1(x_{i-\frac{1}{2}}, y_j) \int_{y_{i-\frac{1}{2}}}^{y_{i+\frac{1}{2}}} (\frac{\xi^n + \xi^{n-1}}{2})_x (x_{i-\frac{1}{2}}, y) dy \Bigg] \\
& + \frac{\Delta t}{4} \Bigg[\bar{g}_1(x_{i+\frac{1}{2}}, y_j) \bar{g}_2(x_i, y_{j+\frac{1}{2}}) \frac{\partial^2(\eta^n - \eta^{n-1})}{\partial x \partial y} (x_{i+\frac{1}{2}}, y_{j+\frac{1}{2}}) \\
& - \bar{g}_1(x_{i+\frac{1}{2}}, y_j) \bar{g}_2(x_i, y_{j-\frac{1}{2}}) \frac{\partial^2(\eta^n - \eta^{n-1})}{\partial x \partial y} (x_{i+\frac{1}{2}}, y_{j-\frac{1}{2}}) \\
& - \bar{g}_1(x_{i-\frac{1}{2}}, y_j) \bar{g}_2(x_i, y_{j+\frac{1}{2}}) \frac{\partial^2(\eta^n - \eta^{n-1})}{\partial x \partial y} (x_{i-\frac{1}{2}}, y_{j+\frac{1}{2}}) \\
& + \bar{g}_1(x_{i-\frac{1}{2}}, y_j) \bar{g}_2(x_i, y_{j-\frac{1}{2}}) \frac{\partial^2(\eta^n - \eta^{n-1})}{\partial x \partial y} (x_{i-\frac{1}{2}}, y_{j-\frac{1}{2}}) \Bigg] \\
& = R_{12}^{n-\frac{1}{2}} + R_4^{n-\frac{1}{2}} + R_5^{n-\frac{1}{2}} + R_6^{n-\frac{1}{2}} + R_{23}^{n-\frac{1}{2}},
\end{aligned}
\tag{20}
$$

where

$$R_{23}^{n-\frac{1}{2}} = \frac{\Delta t}{2}\left[-\int_{x_{i-\frac{1}{2}}}^{x_{i+\frac{1}{2}}} \bar{h}_2(x_i, y_{j-\frac{1}{2}})(R_2^{n-\frac{1}{2}} + R_3^{n-\frac{1}{2}})_y(x, y_{j-\frac{1}{2}})dx \right.$$
$$+ \int_{x_{i-\frac{1}{2}}}^{x_{i+\frac{1}{2}}} \bar{h}_2(x_i, y_{j+\frac{1}{2}})(R_2^{n-\frac{1}{2}} + R_3^{n-\frac{1}{2}})_y(x, y_{j+\frac{1}{2}})dx$$
$$+ \int_{y_{j-\frac{1}{2}}}^{y_{j+\frac{1}{2}}} \bar{h}_1(x_{i+\frac{1}{2}}, y_j)(R_2^{n-\frac{1}{2}} + R_3^{n-\frac{1}{2}})_x(x_{i+\frac{1}{2}}, y)dy$$
$$\left. - \int_{y_{j-\frac{1}{2}}}^{y_{j+\frac{1}{2}}} \bar{h}_1(x_{i-\frac{1}{2}}, y_j)(R_2^{n-\frac{1}{2}} + R_3^{n-\frac{1}{2}})_x(x_{i-\frac{1}{2}}, y)dy\right].$$

Multiply the two sides of Eq. (20) by $\frac{\eta_{ij}^n+\eta_{ij}^{n-1}}{2}$, and add from 1 to $N_x - 1$, $N_y - 1$ for i, j, respectively. Denote the terms of the left hand side of the result by L_1, L_2, L_3, L_4 and the terms of the right hand side by T_1, T_2, T_3, T_4, T_5 sequentially.

Denote $\|\cdot\|_s$ and $|\cdot|_s$ as continuous norm and continuous semi-norm of orders in Sobolev space respectively. Further define the discrete H^1 semi-norm and the discrete L^2 norm respectively by norm respectively by

$$|\phi_h|_{1,h}^2 = \sum_{E\in Q_h} |\phi_h|_{1,h,E}^2, \forall \phi_h \in U_h,$$

$$\|\phi_h\|_{0,h}^2 = \sum_{E\in Q_h} \|\phi_h\|_{0,h,E}^2, \forall \phi_h \in U_h,$$

where $E = \overline{P_1P_2P_3P_4} = [x_{i-1}, x_i] \times [y_{j-1}, y_j]$, depicted as in Fig. 1 and $P_5 = P_1$,

$$|\phi_h|_{1,h,E}^2 = \frac{h_j^y}{2h_i^x} \sum_{l=1,3} (\phi_h(P_{l+1} - \phi_h(P_l)))^2 + \frac{h_i^x}{2h_j^y} \sum_{l=2,4} (\phi_h(P_{l+1} - \phi_h(P_l)))^2,$$

$$\|\phi_h\|_{0,h,E}^2 = \frac{h_i^x h_j^y}{4} \sum_{l=1}^{4} \phi_h(P_l)^2.$$

Lemma 1 [Wang (2008)] For $\forall \phi_h, \varphi_h \in U_h$, denote by

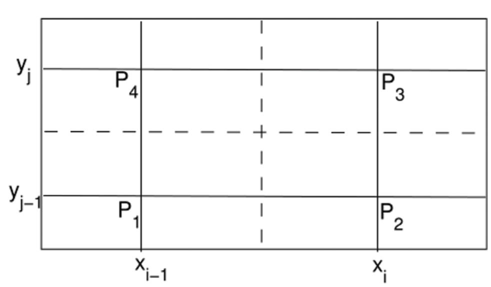

Figure 1: Illustration for an element E and its nodes

$$\phi_{ij} = \phi_h(x_i, y_j), \varphi_{ij} = \varphi_h(x_i, y_j), \|\phi_h\|\|_{0,h}^2 = \sum_{i=1}^{N_x-1}\sum_{j=1}^{N_y-1} \phi_{ij} \iint_{\Omega_{ij}^*} \phi_h dxdy,$$

then

$$\sum_{i=1}^{N_x-1}\sum_{j=1}^{N_y-1} \left[\varphi_{ij} \iint_{\Omega_{ij}^*} \phi_h dxdy - \phi_{ij} \iint_{\Omega_{ij}^*} \varphi_h dxdy\right] = 0, \quad \|\phi_h\|\|_{0,h} \geq \frac{1}{2}\|\phi_h\|_{0,h}.$$

Lemma 2 [Wang (2008)] For $\forall \phi_h, \varphi_h \in U_h$, denote by

$$\|\phi_h\|_{1,h}^2 = -\sum_{i=1}^{N_x-1}\sum_{j=1}^{N_y-1} \phi_{ij} \int_{\partial\Omega_{ij}^*} \frac{\partial \phi_h}{\partial v} ds$$

then

$$\sum_{i=1}^{N_x-1}\sum_{j=1}^{N_y-1} \left[\varphi_{ij} \int_{\partial\Omega_{ij}^*} \frac{\partial \phi_h}{\partial v} ds - \phi_{ij} \int_{\partial\Omega_{ij}^*} \frac{\partial \varphi_h}{\partial v} ds\right] = 0, \quad \|\phi_h\|\|_{1,h}^2 \geq \frac{1}{2}|\phi_h|_{1,h}^2$$

Lemma 3 [Wang (2008)] For $\forall \phi_h, \varphi_h \in U_h$, We have

$$\sum_{i=1}^{N_x-1}\sum_{j=1}^{N_y-1} \varphi_{ij} \left[\frac{\partial^2 \phi_h}{\partial x \partial y}(x_{i+\frac{1}{2}}, y_{j+\frac{1}{2}}) - \frac{\partial^2 \phi_h}{\partial x \partial y}(x_{i+\frac{1}{2}}, y_{j-\frac{1}{2}}) - \frac{\partial^2 \phi_h}{\partial x \partial y}(x_{i-\frac{1}{2}}, y_{j+\frac{1}{2}})\right.$$
$$\left. + \frac{\partial^2 \phi_h}{\partial x \partial y}(x_{i-\frac{1}{2}}, y_{j-\frac{1}{2}})\right] = \sum_{E \in Q_h} \frac{\partial^2 \phi_h}{\partial x \partial y}(x_{i-\frac{1}{2}}, y_{j-\frac{1}{2}}) \frac{\partial^2 \varphi_h}{\partial x \partial y}(x_{i-\frac{1}{2}}, y_{j-\frac{1}{2}}) h_i^x h_j^y.$$

where $E = [x_{i-1}, x_i] \times [y_{j-1}, y_j]$ is an arbitrary element.

Now we estimate L_1, L_2, L_3, L_4. For L_1 and L_2, we have

$$\begin{aligned} L_1 &= \sum_{i=1}^{N_x-1}\sum_{j=1}^{N_y-1} \frac{\eta_{ij}^n + \eta_{ij}^{n-1}}{2} \int\int_{\Omega_{ij}^*} \frac{\eta^n - \eta^{n-1}}{\Delta t} dxdy \\ &= \frac{1}{2\Delta t}\left[|||\eta^n|||_{0,h}^2 - |||\eta^{n-1}|||_{0,h}^2\right], \end{aligned} \tag{21}$$

$$\begin{aligned} L_2 = -\sum_{i=1}^{N_x-1}\sum_{j=1}^{N_y-1} \frac{\eta_{ij}^n + \eta_{ij}^{n-1}}{2} &\left[-\bar{q}_2(x_i, y_{j-\frac{1}{2}}) \int_{x_{i-\frac{1}{2}}}^{x_{i+\frac{1}{2}}} (\frac{\eta^n + \eta^{n-1}}{2})_y (x, y_{j-\frac{1}{2}}) dx \right.\\ &+ \bar{q}_2(x_i, y_{j+\frac{1}{2}}) \int_{x_{i-\frac{1}{2}}}^{x_{i+\frac{1}{2}}} (\frac{\eta^n + \eta^{n-1}}{2})_y (x, y_{j+\frac{1}{2}}) dx \\ &+ \bar{q}_1(x_{i+\frac{1}{2}}, y_j) \int_{y_{i-\frac{1}{2}}}^{y_{i+\frac{1}{2}}} (\frac{\eta^n + \eta^{n-1}}{2})_x (x_{i+\frac{1}{2}}, y) dy \\ &\left. - \bar{q}_1(x_{i-\frac{1}{2}}, y_j) \int_{y_{i-\frac{1}{2}}}^{y_{i+\frac{1}{2}}} (\frac{\eta^n + \eta^{n-1}}{2})_x (x_{i-\frac{1}{2}}, y) dy\right]. \end{aligned}$$

Exist constant q, such that

$$\begin{aligned} L_2 &\geq -q\sum_{i=1}^{N_x-1}\sum_{j=1}^{N_y-1}\frac{\eta_{ij}^n+\eta_{ij}^{n-1}}{2}\int_{\partial\Omega_{ij}^*}\frac{1}{2}\frac{\partial(\eta^n+\eta^{n-1})}{\partial v}ds \\ &\geq \frac{q}{2}\left|\frac{\eta^n+\eta^{n-1}}{2}\right|_{1,h}^2. \end{aligned} \tag{22}$$

For L_3,

$$\begin{aligned} L_3 = -\sum_{i=1}^{N_x-1}\sum_{j=1}^{N_y-1}\frac{\eta_{ij}^n+\eta_{ij}^{n-1}}{2}\Bigg[&-\bar{k}_2(x_i,y_{j-\frac{1}{2}})\int_{x_{i-\frac{1}{2}}}^{x_{i+\frac{1}{2}}}(\frac{\xi^n+\xi^{n-1}}{2})_y(x,y_{j-\frac{1}{2}})dx \\ &+\bar{k}_2(x_i,y_{j+\frac{1}{2}})\int_{x_{i-\frac{1}{2}}}^{x_{i+\frac{1}{2}}}(\frac{\xi^n+\xi^{n-1}}{2})_y(x,y_{j+\frac{1}{2}})dx \\ &+\bar{k}_1(x_{i+\frac{1}{2}},y_j)\int_{y_{i-\frac{1}{2}}}^{y_{i+\frac{1}{2}}}(\frac{\xi^n+\xi^{n-1}}{2})_x(x_{i+\frac{1}{2}},y)dy \\ &-\bar{k}_1(x_{i-\frac{1}{2}},y_j)\int_{y_{i-\frac{1}{2}}}^{y_{i+\frac{1}{2}}}(\frac{\xi^n+\xi^{n-1}}{2})_x(x_{i-\frac{1}{2}},y)dy\Bigg]. \end{aligned}$$

Exist constants $a, \tilde{q} > 0$, such that

$$L_3 \geq -(a-\gamma_1\tilde{q})\sum_{i=1}^{N_x-1}\sum_{j=1}^{N_y-1}\frac{\eta_{ij}^n+\eta_{ij}^{n-1}}{2}\int_{\partial\Omega_{ij}^*}\frac{1}{2}\frac{\partial(\xi^n+\xi^{n-1})}{\partial v}ds. \tag{23}$$

From Eq. (18), we know

$$(\frac{\eta^n+\eta^{n-1}}{2})_{ij} = (\frac{\xi^n-\xi^{n-1}}{\Delta t})_{ij} + \gamma_1(\frac{\xi^n+\xi^{n-1}}{2})_{ij} - R_{2,ij}^{n-\frac{1}{2}}.$$

Put the above formula to Eq. (23), then

$$\begin{aligned} L_3 &\geq -(a-\gamma_1\tilde{q})\sum_{i=1}^{N_x-1}\sum_{j=1}^{N_y-1}\frac{\eta_{ij}^n+\eta_{ij}^{n-1}}{2}\int_{\partial\Omega_{ij}^*}\frac{1}{2}\frac{\partial(\xi^n+\xi^{n-1})}{\partial v}ds \\ &= \gamma_1(a-\gamma_1\tilde{q})|||\frac{\xi^n+\xi^{n-1}}{2}|||_{1,h}^2 + \frac{a-\gamma_1\tilde{q}}{2\Delta t}[|||\xi^n|||_{1,h}^2 - |||\xi^{n-1}|||_{1,h}^2] + L_{31}, \end{aligned} \tag{24}$$

where

$$L_{31}=(a-\gamma_1\tilde{q})\sum_{i=1}^{N_x-1}\sum_{j=1}^{N_y-1}R_{2,ij}^{n-\frac{1}{2}}\int_{\partial\Omega_{ij}^*}\frac{1}{2}\frac{\partial(\xi^n+\xi^{n-1})}{\partial v}ds.$$

Using Cauchy inequality, we have

$$|L_{31}|\le C|R_2^{n-\frac{1}{2}}|_{1,h}^2+\epsilon|\frac{\xi^n+\xi^{n-1}}{2}|_{1,h}^2\le C\Delta t^4+\epsilon|\frac{\xi^n+\xi^{n-1}}{2}|_{1,h}^2. \tag{25}$$

For L_4, exist constant g^2, such that

$$\begin{aligned}L_4=&\sum_{i=1}^{N_x-1}\sum_{j=1}^{N_y-1}\frac{\eta_{ij}^n+\eta_{ij}^{n-1}}{2}\frac{\Delta t}{4}\Big[\bar{g}_1(x_{i+\frac{1}{2}},y_j)\bar{g}_2(x_i,y_{j+\frac{1}{2}})\frac{\partial^2(\eta^n-\eta^{n-1})}{\partial x\partial y}(x_{i+\frac{1}{2}},y_{j+\frac{1}{2}})\\&-\bar{g}_1(x_{i+\frac{1}{2}},y_j)\bar{g}_2(x_i,y_{j-\frac{1}{2}})\frac{\partial^2(\eta^n-\eta^{n-1})}{\partial x\partial y}(x_{i+\frac{1}{2}},y_{j-\frac{1}{2}})\\&-\bar{g}_1(x_{i-\frac{1}{2}},y_j)\bar{g}_2(x_i,y_{j+\frac{1}{2}})\frac{\partial^2(\eta^n-\eta^{n-1})}{\partial x\partial y}(x_{i-\frac{1}{2}},y_{j+\frac{1}{2}})\\&+\bar{g}_1(x_{i-\frac{1}{2}},y_j)\bar{g}_2(x_i,y_{j-\frac{1}{2}})\frac{\partial^2(\eta^n-\eta^{n-1})}{\partial x\partial y}(x_{i-\frac{1}{2}},y_{j-\frac{1}{2}})\Big]\\\ge&\frac{g^2\Delta t}{8}\sum_{i=1}^{N_x-1}\sum_{j=1}^{N_y-1}(\eta_{ij}^n+\eta_{ij}^{n-1})\Big[\frac{\partial^2(\eta^n-\eta^{n-1})}{\partial x\partial y}(x_{i+\frac{1}{2}},y_{j+\frac{1}{2}})\\&-\frac{\partial^2(\eta^n-\eta^{n-1})}{\partial x\partial y}(x_{i+\frac{1}{2}},y_{j-\frac{1}{2}})-\frac{\partial^2(\eta^n-\eta^{n-1})}{\partial x\partial y}(x_{i-\frac{1}{2}},y_{j+\frac{1}{2}})\\&+\frac{\partial^2(\eta^n-\eta^{n-1})}{\partial x\partial y}(x_{i-\frac{1}{2}},y_{j-\frac{1}{2}})\Big].\end{aligned}$$

By Lemma 3, we obtain

$$L_4\ge\frac{g^2\Delta t}{8}\Big[\|\frac{\partial^2\eta^n}{\partial x\partial y}\|_{0,h}^2-\|\frac{\partial^2\eta^{n-1}}{\partial x\partial y}\|_{0,h}^2\Big]. \tag{26}$$

To estimate T_1, using Cauchy inequality, we see that

$$\begin{aligned}|T_1|&=|\sum_{i=1}^{N_x-1}\sum_{j=1}^{N_y-1}\frac{\eta_{ij}^n+\eta_{ij}^{n-1}}{2}R_{12}^{n-\frac{1}{2}}|\\&\le C\|\frac{\eta^n+\eta^{n-1}}{2}\|_{0,h}^2+C\Delta t^3\int_{t^{n-1}}^{t^n}\Big[\|u_{tt}\|_2^2+\|v_{tt}\|_2^2\Big]dt.\end{aligned} \tag{27}$$

To estimate T_2, using finite element interpolation error estimates, we have

$$|T_2| \le C\|\frac{\eta^n+\eta^{n-1}}{2}\|_{0,h}^2 + \frac{Ch^4}{\Delta t}\int_{t^{n-1}}^{t^n}\|v_t\|_2^2dt$$

$$\begin{aligned}|T_2| &\le C\|\frac{\eta^n+\eta^{n-1}}{2}\|_{0,h}^2 + \frac{Ch^4}{\Delta t}\int_{t^{n-1}}^{t^n}\|v_t\|_2^2dt \\ &+\epsilon|\frac{\eta^n+\eta^{n-1}}{2}|_{1,h}^2 + Ch^4\left[|u^{n-1}|_3^2 + |v^n+v^{n-1}|_3^2\right].\end{aligned} \tag{28}$$

where $|u|_3 = \left(\sum_{|\alpha|=3}\|D^\alpha u(x,y)\|_0^2\right)^{\frac{1}{2}}$.

For the integral approximation error T_3, using *Lipschitz* condition and interpolation error estimates, we can prove that

$$\begin{aligned}|T_3| &\le C\|\frac{\eta^n+\eta^{n-1}}{2}\|_{0,h}^2 + C\sum_{i=1}^{N_x-1}\sum_{j=1}^{N_y-1}(R_5^{n-\frac{1}{2}})^2 \\ &\le C\|\frac{\eta^n+\eta^{n-1}}{2}\|_{0,h}^2 + Ch^4|\frac{v^n+v^{n-1}}{2}|_3^2 + Ch^4|u^{n-1}|_3^2.\end{aligned} \tag{29}$$

Next, we estimate disturbance error T_4, we can see that

$$\begin{aligned}|T_4| &\le C\Delta t^3\int_{t^{n-1}}^{t^n}\|v_t\|_4^2dt + C\Delta t^3\int_{t^{n-1}}^{t^n}\int\int_{\Omega^*}(\frac{\partial^5 v}{\partial x^2\partial y^2\partial t})^2dxdydt \\ &+\epsilon|\frac{\eta^n+\eta^{n-1}}{2}|_1^2 + C\|\frac{\eta^n+\eta^{n-1}}{2}\|_{0,h}^2.\end{aligned} \tag{30}$$

We estimate the last term T_5

$$\begin{aligned}|T_5| &\le C\Delta t\Big\{\|\frac{\eta^n+\eta^{n-1}}{2}\|_{0,h}^2 + \epsilon|\frac{\eta^n+\eta^{n-1}}{2}|_1^2 + C\Delta t^3\int_{t^{n-1}}^{t^n}[\|u_{tt}\|_2^2+\|v_{tt}\|_2^2]dt \\ &+C\frac{h^4}{\Delta t}\int_{t^{n-1}}^{t^n}|u_t|_3^2dt + Ch^4|\frac{u^n+u^{n-1}}{2}|_3^2 + Ch^4|\frac{v^n+v^{n-1}}{2}|_3^2\Big\}.\end{aligned} \tag{31}$$

Combining the equations from Eqs. (21) to (31) with Eq. (20) and Lemma 1,2, we conclude that

$$\begin{aligned}
&\frac{1}{2\Delta t}\Big[|\parallel \eta^n \parallel|_{0,h}^2 - |\parallel \eta^{n-1} \parallel|_{0,h}^2\Big] + \frac{q}{2}\Big|\frac{\eta^n + \eta^{n-1}}{2}\Big|_{1,h}^2 + \gamma_1(a-\gamma_1\tilde{q})|\parallel \frac{\xi^n + \xi^{n-1}}{2} \parallel|_{1,h}^2 \\
&\quad + \frac{a-\gamma_1\tilde{q}}{2\Delta t}\Big[|\parallel \xi^n \parallel|_{1,h}^2 - |\parallel \xi^{n-1} \parallel|_{1,h}^2\Big] + \frac{g^2\Delta t}{8}\Big[\parallel \frac{\partial^2\eta^n}{\partial x\partial y}\parallel_{0,h}^2 - \parallel \frac{\partial^2\eta^{n-1}}{\partial x\partial y}\parallel_{0,h}^2\Big] \\
&\quad \le C\Delta t^4 + C\Delta t^3\int_{t^{n-1}}^{t^n}\big[\parallel u_{tt}\parallel_2^2 + \parallel v_{tt}\parallel_2^2\big] + C\Delta t^3\int_{t^{n-1}}^{t^n}\parallel v_t\parallel_4^2\,dt \\
&\quad + C\Delta t^3\int_{t^{n-1}}^{t^n}\int\int_{\Omega^*}\Big(\frac{\partial^5 v}{\partial x^2\partial y^2\partial t}\Big)^2 dxdydt + \frac{Ch^4}{\Delta t}\int_{t^{n-1}}^{t^n}\parallel v_t\parallel_2^2\,dt \\
&\quad + Ch^4\Big[|u^{n-1}|_3^2 + |v^n + v^{n-1}|_3^2\Big] + C\frac{h^4}{\Delta t}\int_{t^{n-1}}^{t^n}|u_t|_3^2 dt \\
&\quad + Ch^4\Big|\frac{u^n + u^{n-1}}{2}\Big|_3^2 + Ch^4\Big|\frac{v^n + v^{n-1}}{2}\Big|_3^2 \\
&\quad + \epsilon\Big|\frac{\eta^n + \eta^{n-1}}{2}\Big|_{1,h}^2 + C\parallel \frac{\eta^n + \eta^{n-1}}{2}\parallel_{0,h}^2 .
\end{aligned} \tag{32}$$

Multiplying by $2\Delta t$, adding over n, using discrete Gronwall Lemma and equivalence relations between continuous norm and the corresponding discrete norm, we obtain

$$\|\eta^n\|_0 + |\xi^n|_1 \le C(\Delta t^2 + h^2).$$

Using interpolation approximation theorem in Sobolev space and equivalence relations between H^1norm and H^1 semi-norm in $H_0^1(\Omega)$, we have

$$\|u^n - u_h^n\|_0 + \|v^n - v_h^n\|_0 \le C(\Delta t^2 + h^2). \tag{33}$$

Theorem 1 Let $u, v \in H^2(0, T; H_0^1(\Omega)\bigcap_{H^3}(\Omega))$ be the solutions of the differential Eq. (2) and u_h, v_h the solutions of the numerical schemes Eqs. (14) and (16), then the following estimate holds:

$$\|u^n - u_h^n\|_0 + \|v^n - v_h^n\|_0 \le C(\Delta t^2 + h^2). \tag{34}$$

2 Numerical experiments

In this section, we give four numerical experiments: two numerical examples with constant coefficients and two numerical examples with variable coefficients. From these examples, we verify the effectiveness of the schemes in this article. For the purpose of checking numerical errors of algorithms for solving (1), four problems possessing exact solutions are considered. In all numerical experiments, the special domain is $\Omega=(0,1)\times(0,1)$and the time interval is J=(0, 1]. Finally, we point out that all numerical experiments are done with Matlab.

2.1 Experiment 1

In the first problem, we select $\gamma_1=1, Q=A=I$. The following function

$u(x, y, t) = \left[1 + 0.5\sin(\pi^2 t)\right]\sin(5\pi x)\sin(3\pi y), (x, y, t) \in \Omega \times J$

is selected as an exact solution. The source is given as

$S(x, y, t) = \pi^2 \sin(5\pi x)\sin(3\pi y)\left[34 + (0.5 + 17\pi^2)\cos(\pi^2 t) + (17 - 0.5\pi^2)\sin(\pi^2 t)\right].$

The numerical results are as follows:

Figs. 2-4 presents numerical solution and exact solution of u, as well as the L^2 error between them in experiment 1 (case $h = 0.025, \Delta t = 0.025$). Tab. 1 presents the maximum absolute error $L^\infty$and the convergence rate m. The error L^∞ is the maximum absolute error of the computed solution with respect to the exact solution at the final time T=1. As the table shows, the algorithm has a second-order accuracy, which confirms the theoretical results. Errors measured in the L^2 norm showed similar results. As one can see from Tab. 2, our algorithm shows higher accuracy than the algorithm based on the discretization scheme in Zampieri et al. [Zampieri and Pavarino (2006)]. Tab. 3 shows the accuracy of our method (ADI-FVEM) and finite volume element method (FVEM) gradually decreases with decrease of time step and space step, but they have the same order. In Tab. 3, we further list the CPU times of our schemes and finite volume element schemes. From Fig. 5, we see ADI-FVEM is more efficient than FVEM with the increase of computing scale.

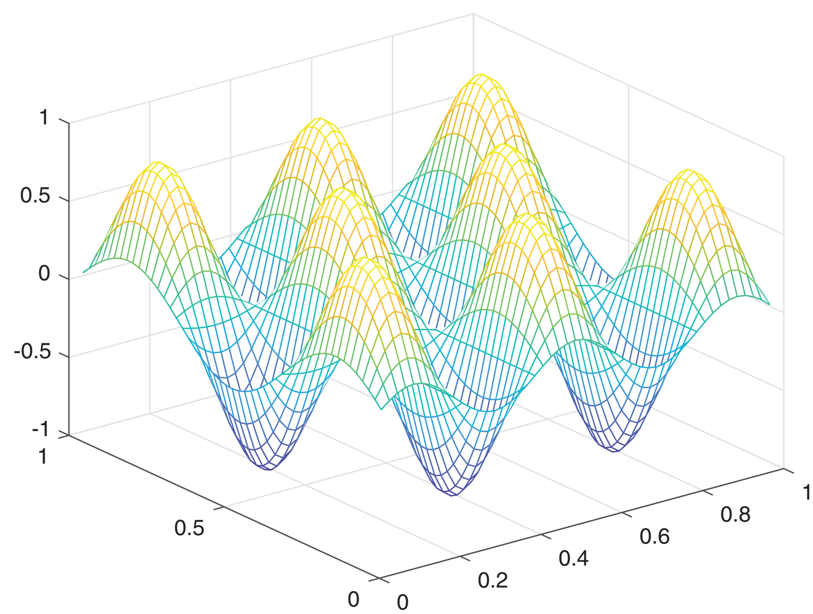

Figure 2: Numerical solution of u in experiment 1 (case $h = 0.02, \Delta t = 0.02$)

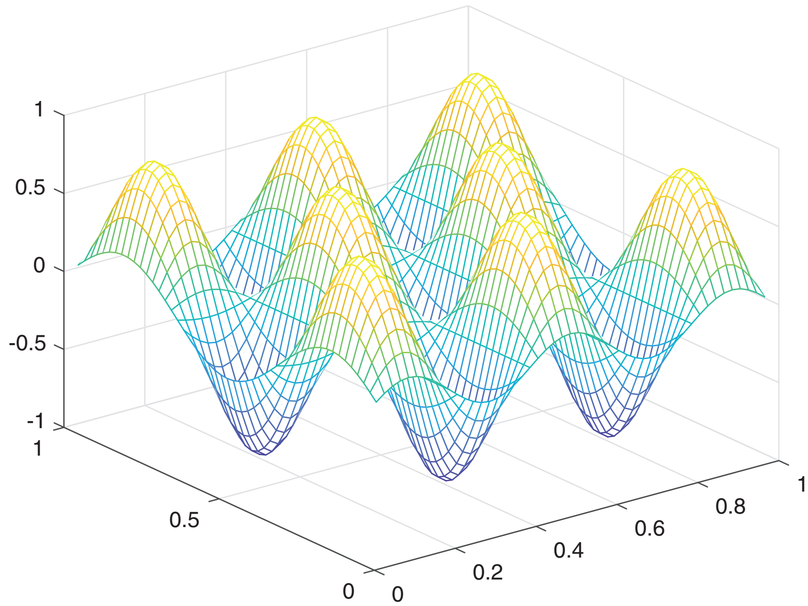

Figure 3: Exact solution of u in experiment 1 (case $h=0.02, \Delta t=0.02$)

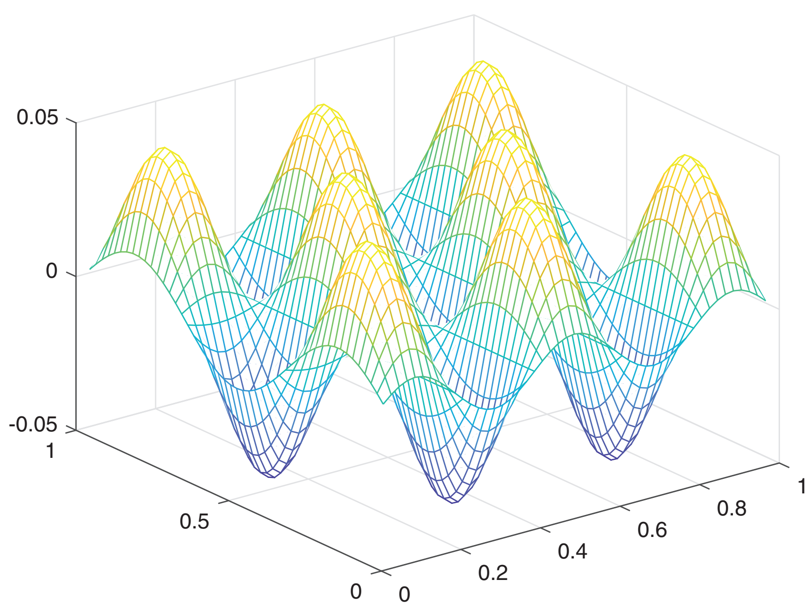

Figure 4: L^2 error between numerical solution and exact solution of u in experiment 1 (case $h=0.02, \Delta t=0.02$)

Table 1: Maximum absolute error L^∞, L^2 and their convergence rates

$(h, \Delta t)$	L^∞	**m**	L^2	**m**
(0.02,0.02)	4.590E-2		2.295E-2	
(0.01,0.01)	1.126E-2	2.0187	5.631E-3	2.0187
(0.005,0.005)	2.801E-3	2.0052	1.401E-3	2.0052

Table 2: Maximum absolute error L^∞ and convergence rate

$(h, \Delta t)$	L^∞	**m**	**Zampieri et al. (2006)** ***Scheme*** L^∞	**m**
(0.02,0.02)	4.59E-2		3.48E-1	
(0.01,0.01)	1.13E-2	2.0187	1.13E-1	1.62
(0.005,0.005)	2.80E-3	2.0052	4.27E-2	1.40

Table 3: Maximum absolute error L^∞ and CPU times of ADI-FVEM and FVEM

Index	$(h, \Delta t)$	**ADI-FVEM**		**FVEM**	
		L^∞	*CPU*	L^∞	*CPU*
1	(0.02,0.02)	4.590E-2	15.703s	3.379E-3	22.975s
2	(0.01,0.01)	1.126E-2	581.588s	8.427E-4	2331.732s
3	(0.005,0.005)	2.801E-3	20334.558s	2.105E-4	89623.054s

2.2 Experiment 2

In the second problem, we select $\gamma_1 = 10, Q = 0$ and $A = I$. We choose the following function

$$u(x, y, t) = e^{-vt} \sin(v_t t) \sin(v_x x) \sin(v_y y), (x, y, t) \in \Omega \times J$$

as an exact solution, where v, v_t, v_x, v_y are constants. The source is given as

$$S(x, y, t) = \sin(v_x x) \sin(v_y y) \left[(-v + v^2 - v_t^2 - v_x^2 - v_y^2) e^{vt} \sin(v_t t) + (v_t - 2vv_t) \cos(v_t t)\right].$$

The numerical results are as follows:

Figs. 6-8 presents numerical solution and exact solution of u, as well as the L^2 error between them in experiment 2 (case $(a) v = -\pi/2$, and $h = 0.025, \Delta t = 0.01$). Figs. 10-12 presents numerical solution and exact solution of u, as well as the L^2 error between them in experiment 2 (case $(b) v = \pi/2$, and $h = 0.025, \Delta t = 0.01$). Tabs. 4 and 5 show a second-order accuracy in $(a) v = -\pi/2$, $v_t = 2\pi$, $v_x = v_y = 4\pi$ and $(b) v = \pi/2$, $v_t = 2\pi$, $v_x = v_y = 4\pi$,

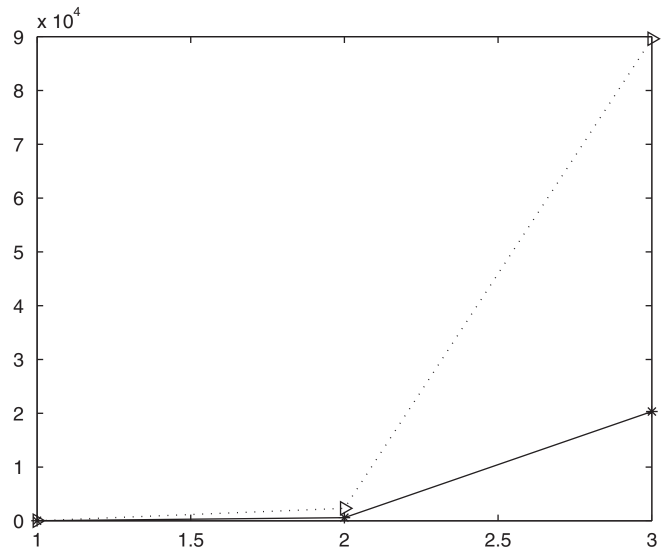

Figure 5: Comparison of CPU times of ADI-FVEM and FVEM in experiment 1. The dashed line ▹ represents CPU times of FVEM, while The solid line $*$ is CPU times of ADI-FVEM is CPU times of ADI-FVEM

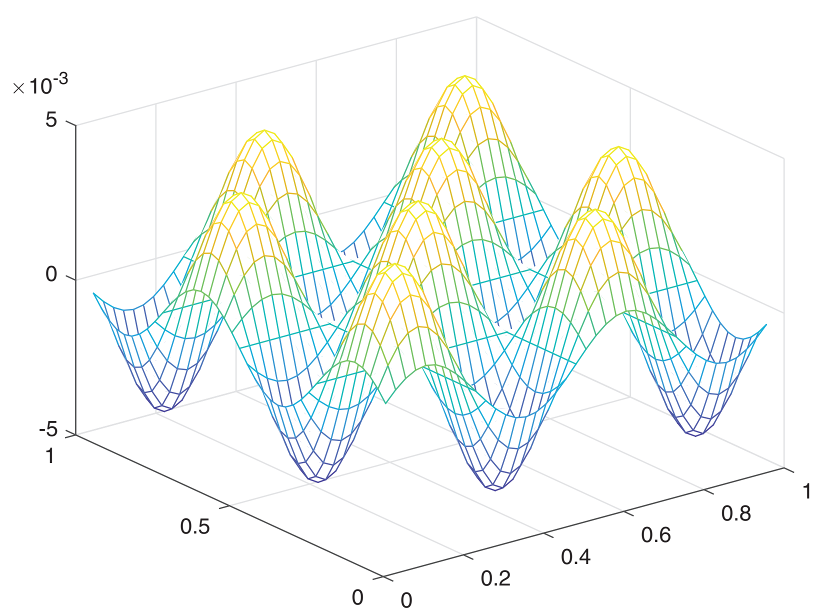

Figure 6: Numerical solution of u in experiment 2(a) (case $h = 0.025, \Delta t = 0.01$)

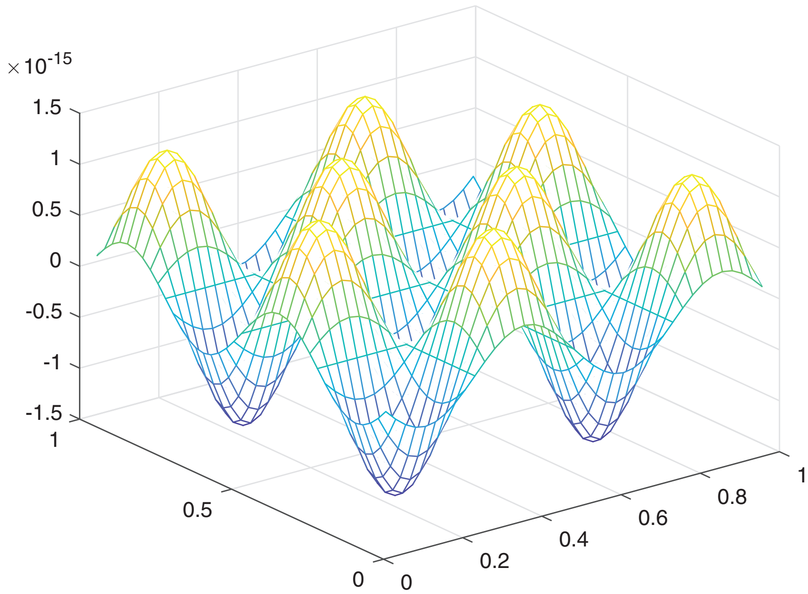

Figure 7: Exact solution of u in experiment 2(a) (case $h = 0.025, \Delta t = 0.01$)

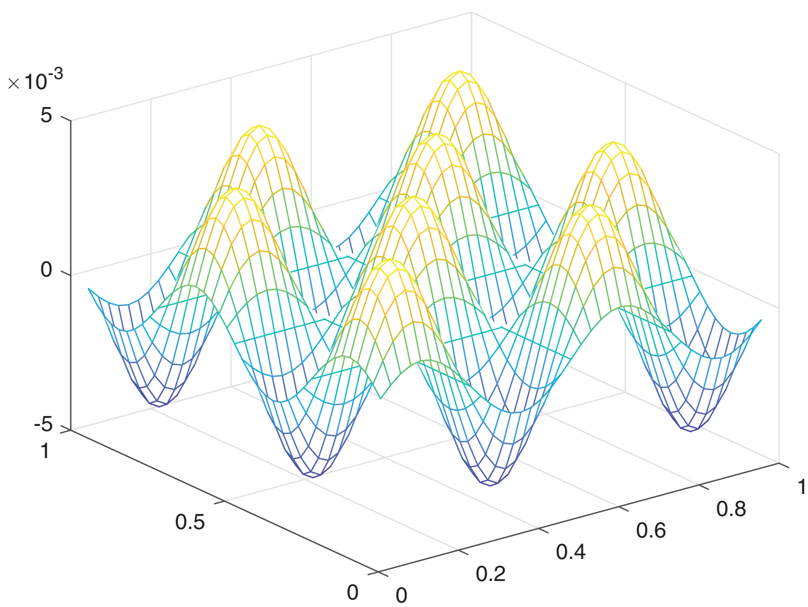

Figure 8: L^2 error between numerical solution and exact solution of u in experiment 2(a) (case $h = 0.025, \Delta t = 0.01$)

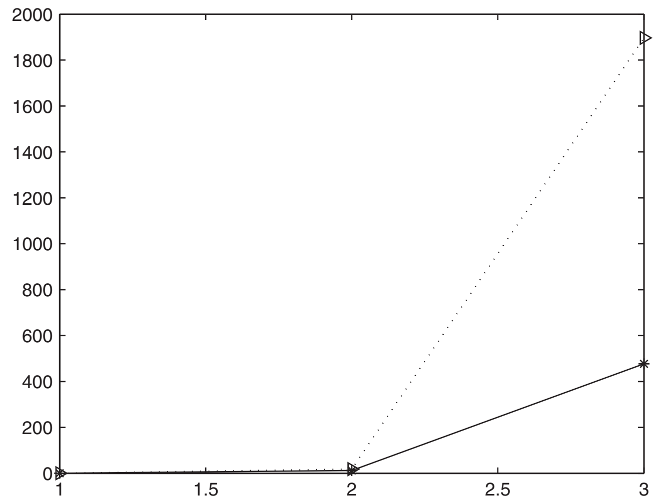

Figure 9: Comparison of CPU times of ADI-FVEM and FVEM in experiment 2(a) $v=-\pi/2$. The dashed line $\triangleright$ represents CPU times of FVEM, while The solid line $*$ is CPU times of ADI-FVEM

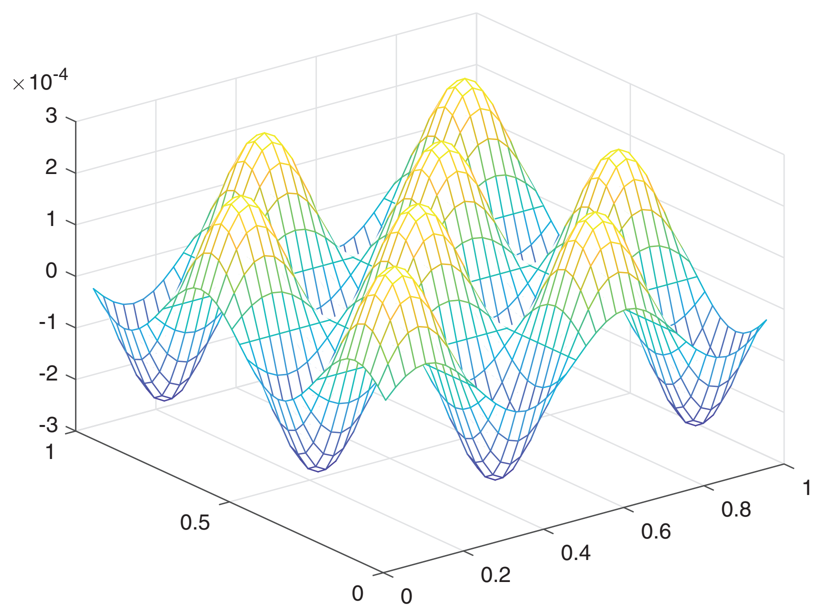

Figure 10: Numerical solution of u in experiment 2(b) (case $h=0.025, \Delta t=0.01$)

which confirms the theoretical results. In Tabs. 6 and 7, the accuracy of the ADI-FVEM and the FVEM schemes are almost the same, but we see ADI-FVEM is more efficient than FVEM with the increase of computing scale from Figs. 9 and 13.

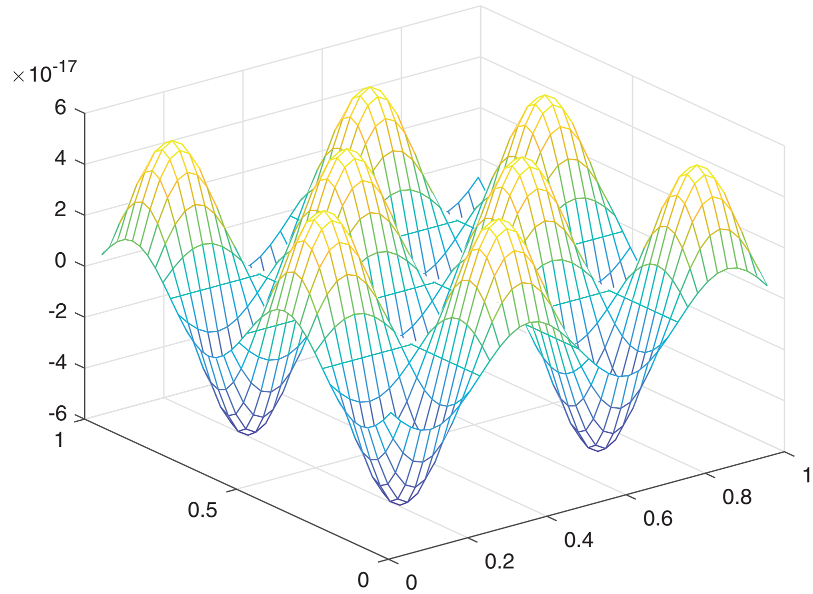

Figure 11: Numerical solution of u in experiment 2(b) (case $h = 0.025, \Delta t = 0.01$)

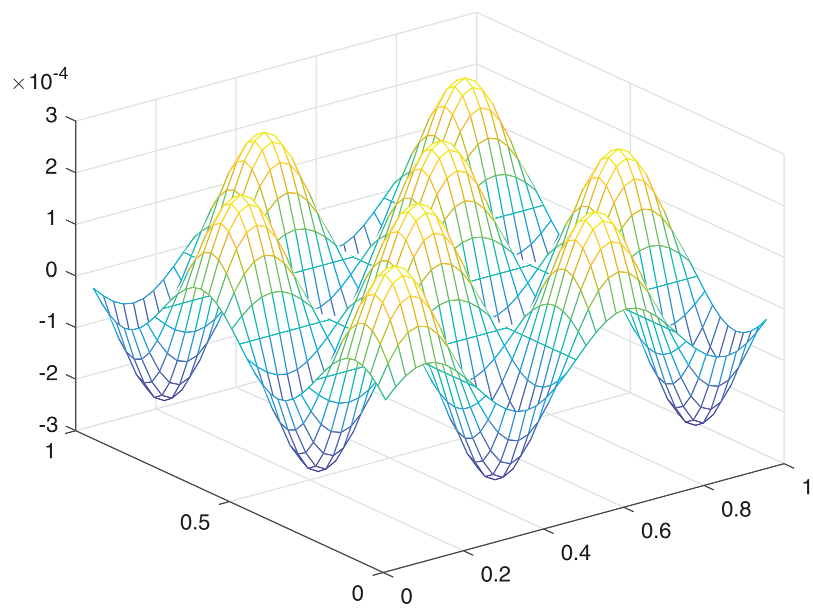

Figure 12: L^2 error between numerical solution and exact solution of u in experiment 2(b) (case $h = 0.025, \Delta t = 0.01$)

Table 4: Maximum absolute error L^∞, L^2 and their convergence rates in (a)

$(h, \Delta t)$	L^∞	**m**	L^2	**m**
$(0.05, 0.02)$	1.464E-2		8.0925E-3	
$(0.025, 0.01)$	4.110E-3	1.8874	2.0589E-3	1.9845
$(0.0125, 0.005)$	1.031E-3	1.9965	2.9078E-5	1.9965

Table 5: Maximum absolute error L^∞, L^2 and their convergence rates in (b)

$(h, \Delta t)$	L^∞	**m**	L^2	**m**
$(0.05, 0.02)$	8.611E-4		4.7602E-4	
$(0.025, 0.01)$	2.337E-4	1.9197	1.1684E-4	2.0185
$(0.0125, 0.005)$	5.816E-5	2.0045	2.9078E]-5	2.0045

2.3 Experiment 3

In the third problem, we select $\gamma_1 = 1, Q = diag(x, y), A = diag(x, y)$. We choose the following function

$u(x, y, t) = e^{-t} \sin(\pi x) \sin(\pi y), (x, y, t) \in \Omega \times J$

as an exact solution.The source is given as

$S(x, y, t) = 0.$

The numerical results are as follows:

Figs. 14-16 presents numerical solution and exact solution of u, as well as the L^2 error between them in experiment 3 (case $h = 0.025, \Delta t = 0.01$). Tab. 8 presents a second-order accuracy in L^2 norm and L^∞ norm, which confirms the theoretical results. In Tab. 9, the accuracy of the ADI-FVEM and FVEM schemes are almost the same, but we see ADI-FVEM is more efficient than FVEM with the increase of computing scale from Fig. 17.

Table 6: Maximum absolute error L^∞ and CPU times of ADI-FVEM and FVEM in (a)

Index	$(h, \Delta t)$	**ADI-FVEM**		**FVEM**	
		L^∞	*CPU*	L^∞	*CPU*
1	(0.05,0.02)	1.464E-2	0.377s	1.491E-2	0.418s
2	(0.025,0.01)	4.110E-3	12.560s	4.130E-3	18.341s
3	(0.0125,0.005)	1.031E-3	476.574s	1.032E-3	1896.386s

Table 7: Maximum absolute error L^∞ and CPU times of ADI-FVEM and FVEM in (b)

Index	$(h, \Delta t)$	ADI-FVEM		FVEM	
		L^∞	CPU	L^∞	CPU
	(0.05,0.02)	8.611E-4	0.634s	8.690E-4	0.615s
	(0.025,0.01)	2.337E-4	13.885s	2.342E-4	20.572s
	(0.0125,0.005)	5.816E-5	537.422s	5.819E-5	2905.936s

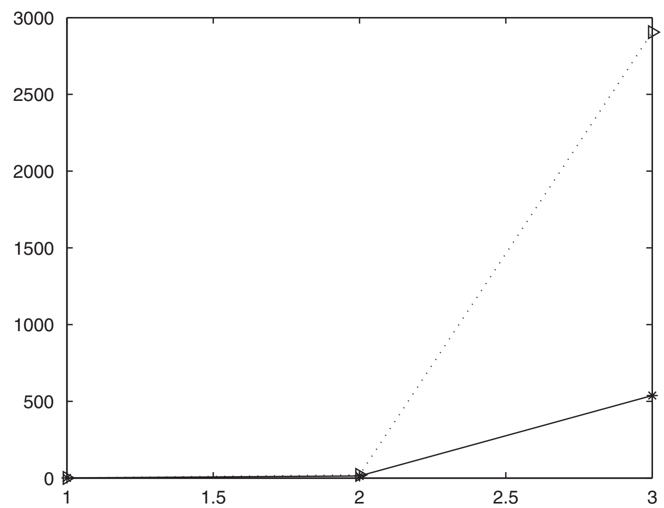

Figure 13: Comparison of CPU times of ADI-FVE and FVEM in experiment 2(b) $v = \pi/2$. The dashed line $\triangleright$ represents CPU times of FVEM, while The solid line $*$ is CPU times of ADI-FVEM

Table 8: Maximum absolute error L^∞, L^2 and their convergence rates

$(h, \Delta t)$	L^∞	**m**	L^2	**m**
$(0.2, 0.2)$	1.114E-3		6.1580E-4	
$(0.1, 0.1)$	3.069E-4	1.9052	1.5345E-4	2.0033
$(0.05, 0.05)$	7.666E-5	2.0008	3.8331E-5	2.0008
$(0.025, 0.025)$	1.916E-5	2.0011	9.5808E-6	2.0002

Table 9: Maximum absolute error L^∞ and CPU times of ADI-FVEM and FVEM

Index	$(h,\Delta t)$	**ADI-FVEM**		**FVEM**	
		L^∞	*CPU*	L^∞	*CPU*
1	$(0.2, 0.2)$	$1.114E$-3	$0.0008s$	$1.114E$-3	$0.0005s$
2	$(0.1, 0.1)$	$3.069E$-4	$0.005s$	$3.069E$-4	$0.027s$
3	$(0.05, 0.05)$	$7.666E$-5	$0.122s$	$7.666E$-5	$1.157s$
4	$(0.025, 0.025)$	$1.916E$-5	$4.352s$	$1.916E$-5	$49.931s$

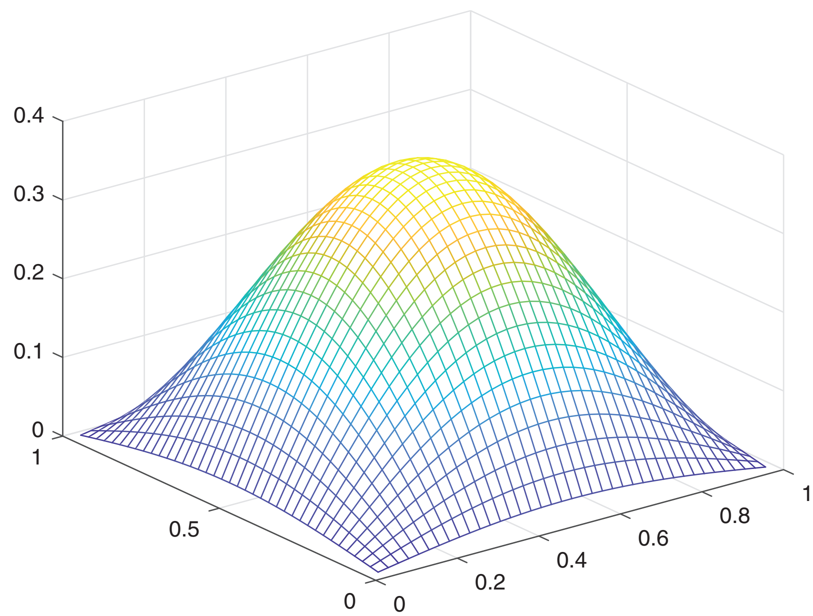

Figure 14: Numerical solution of u in experiment 3 (case $h = 0.025, \Delta t = 0.01$)

2.4 Experiment 4

In the fourth problem, we select $\gamma_1 = 1, Q = diag\{x, y\}, A = diag\{y, x\}$. We choose the following function

$$u(x, y, t) = e^{-t}\sin(\pi x)\sin(\pi y), (x, y, t) \in \Omega \times J$$

as an exact solution.The source is given as

$$S(x, y, t) = \pi e^{-t}\sin[\pi(x + y)].$$

The numerical results are as follows:

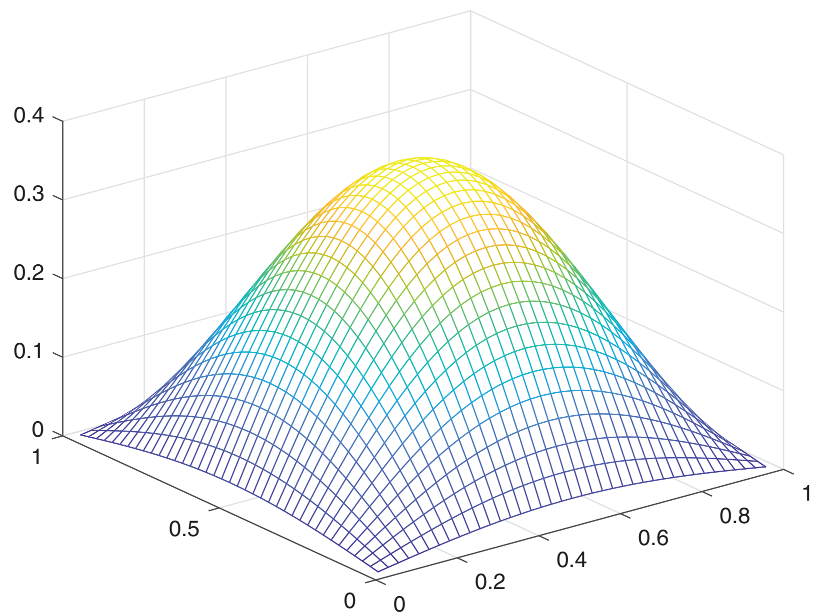

Figure 15: Exact solution of u in experiment 3 (case $h = 0.025, \Delta t = 0.01$)

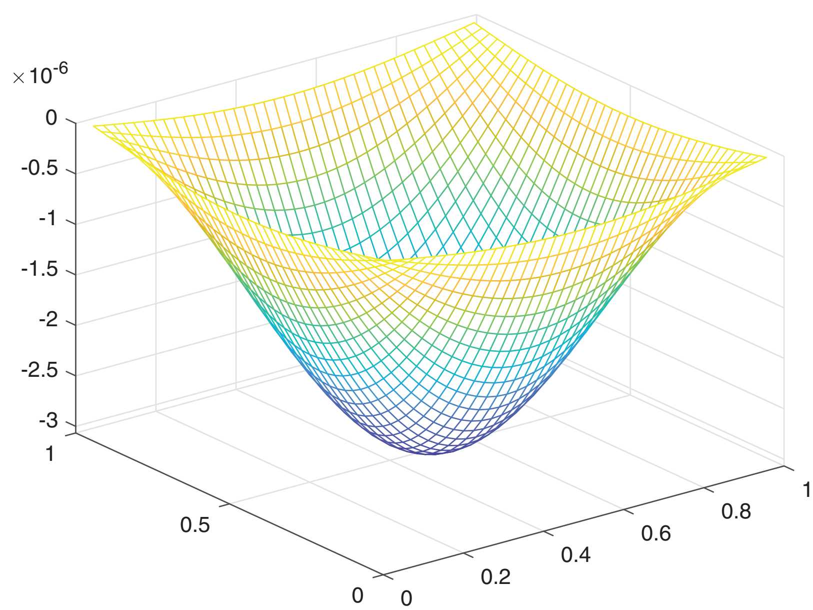

Figure 16: L^2 error between numerical solution and exact solution of u in experiment 3 (case $h = 0.025, \Delta t = 0.01$)

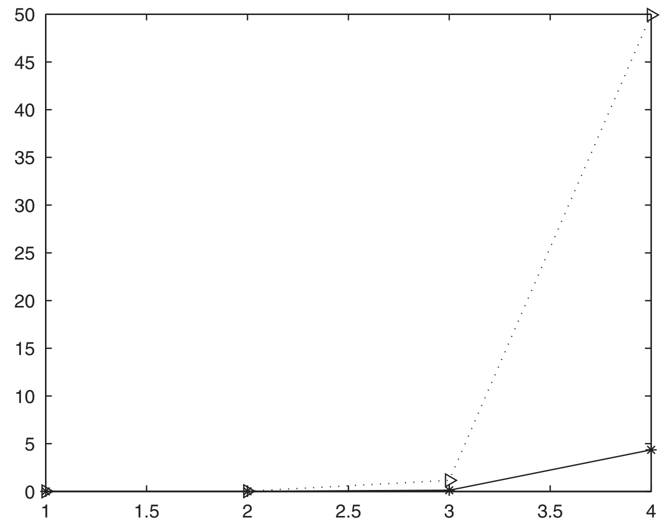

Figure 17: Comparison of CPU times of ADI-FVEM and FVEM in experiment 3. The dashed line ▷ represents CPU times of FVEM, while The solid line * is CPU times of ADI-FVEM

Figs. 18-20 presents numerical solution and exact solution of u, as well as the L^2 error between them in experiment 4 (case $h = 0.025, \Delta t = 0.025$). Tab. 10 presents a second-order accuracy in L^2 norm and L^∞ norm, which confirms the theoretical results. In Tab. 11 the accuracy of the ADI-FVEM and FVEM schemes are almost the same, but we see ADI-FVEM is more efficient than FVEM with the increase of computing scale from Fig. 21.

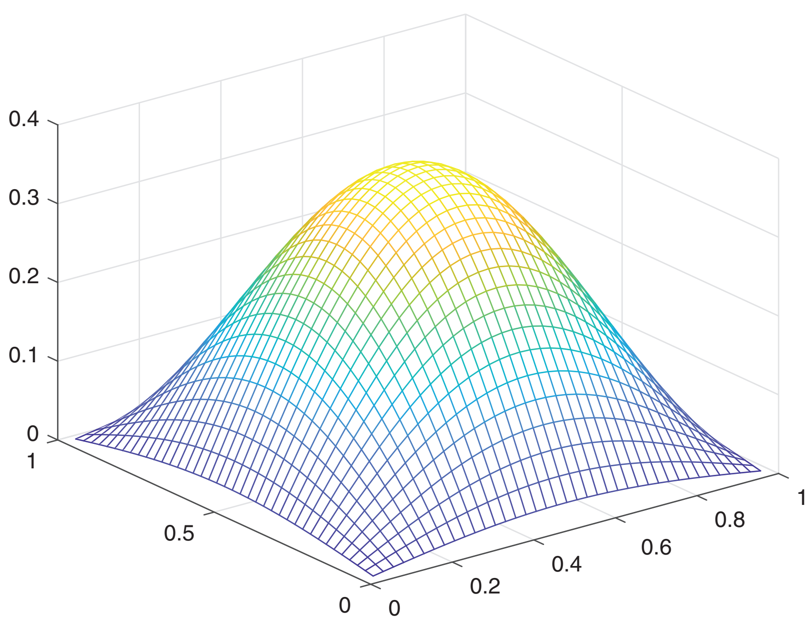

Figure 18: Numerical solution of u in experiment 4 (case $h = 0.025, \Delta t = 0.025$)

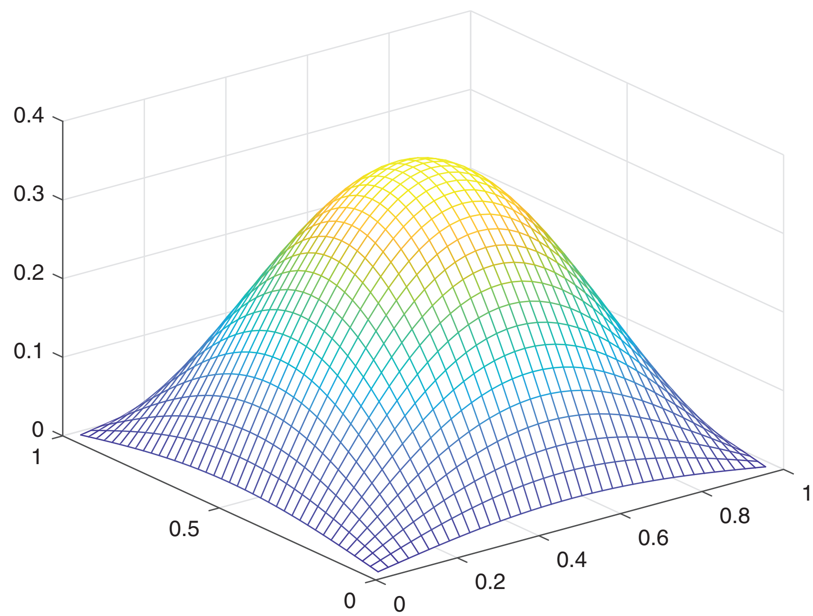

Figure 19: Exact solution of u in experiment 4 (case $h = 0.025, \Delta t = 0.025$)

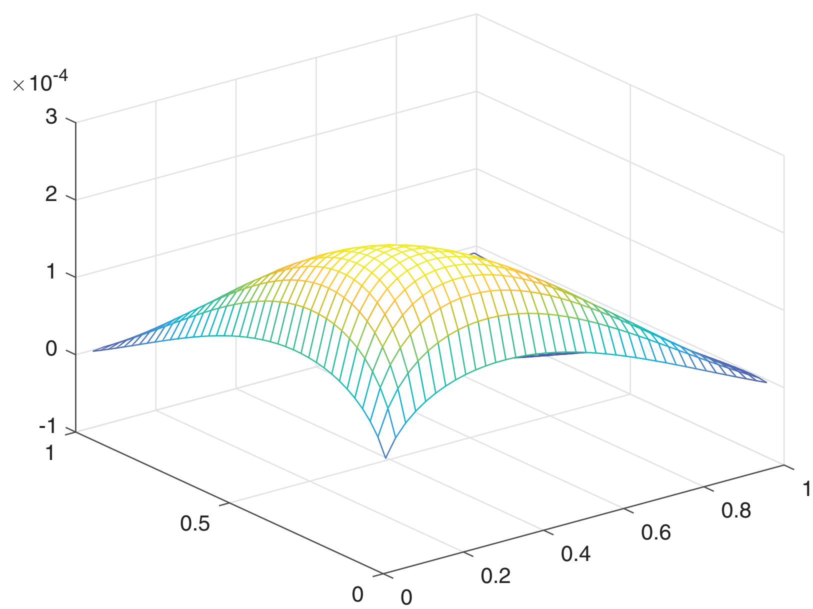

Figure 20: L^2 error between numerical solution and exact solution of u in experiment 4 (case $h = 0.025, \Delta t = 0.025$)

Table 10: Maximum absolute error L^∞ , L^2 and their convergence rates

$(h, \Delta t)$	L^∞	**m**	L^2	**m**
$(0.2, 0.2)$	1.063*E*-2		4.0082*E*-3	
$(0.1, 0.1)$	3.260*E*-3	1.8060	1.3433*E*-3	1.7445
$(0.05, 0.05)$	9.257*E*-4	1.8764	3.8980*E*-4	1.8564
$(0.025, 0.025)$	2.511*E*-4	1.9201	1.0705*E*-4	1.9082

Table 11: Maximum absolute error L^∞ and CPU times of ADI-FVEM and FVEM

Index	$(h, \Delta t)$	**ADI-FVEM**		**FVEM**	
		L^∞	*CPU*	L^∞	*CPU*
1	$(0.2, 0.2)$	1.063*E*-2	0.0009*s*	1.063*E*-2	0.0003*s*
2	$(0.1, 0.1)$	3.259*E*-3	0.011*s*	3.259*E*-3	0.024*s*
3	$(0.05, 0.05)$	9.257*E*-4	0.336*s*	9.257*E*-4	1.147*s*
4	$(0.025, 0.025)$	2.511*E*-4	12.142*s*	2.511*E*-4	42.894*s*

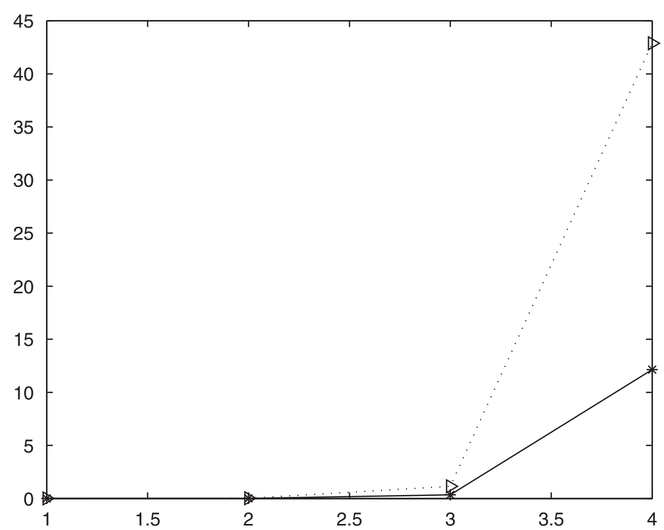

Figure 21: Comparison of CPU times of ADI-FVEM and FVEM in experiment 4. The dashed line ▷ represents CPU times of FVEM, while The solid line * is CPU times of ADI-FVEM

3 Conclusions

In this paper, an alternating-direction implicit finite volume element method was proposed to solve a viscous wave equation with variable coefficients and the error estimate respect to L^2 is derived. Four numerical examples demonstrated the effectiveness of the scheme and the theoretical result. Also, we can see that our approach is more efficient than the standard finite volume element schemes with the increasing scale.

Funding Statement: This work is partially supported by the National Natural Science Foundation of China grants No. 11971241.

Conflicts of Interest: The authors declare that they have no conflicts of interest to report regarding the present study.

References

Bank, R. E.; Rose, D. J. (1987): Some error estimates for the box method. *SIAM Journal on Numerical Analysis*, vol. 24, no. 4, pp. 777-787. DOI 10.1137/0724050.

Cai, Z. (1990): On the finite volume element method. *Numerische Mathematik*, vol. 58, no. 1, pp. 713-735. DOI 10.1007/BF01385651.

Cai, Z.; McCormick, S. (1990): On the accuracy of the finite volume element method for diffusion equations on composite grids. *SIAM Journal on Numerical Analysis*, vol. 27, no. 3, pp. 636-655. DOI 10.1137/0727039.

Celikten, G.; Aksan, E. N. (2019): Alternating direction implicit method for numerical solutions of 2-d burgers equations. *Thermal Science*, vol. 23, no. 1, pp. S243-S252. DOI 10.2298/TSCI181111038C.

Chatzipantelidis, P.; Lazarov, R.; Thomée, V. (2004): Error estimates for a finite volume element method for parabolic equations in convex polygonal domains. *Numerical Methods for Partial Differential Equations: An International Journal*, vol. 20, no. 5, pp. 650-674. DOI 10.1002/num.20006.

Chen, H.; Xu, D.; Cao, J.; Zhou, J. (2018): A backward Euler alternating direction implicit difference scheme for the three-dimensional fractional evolution equation. *Numerical Methods for Partial Differential Equations*, vol. 34, no. 3, pp. 938-958. DOI 10.1002/num.22239.

Chen, H.; Zhou, H.; Jiang, S.; Rao, Y. (2019): Fractional Laplacian viscoacoustic wave equation low-rank temporal extrapolation. *IEEE Access*, vol. 7, pp. 93187-93197. DOI 10.1109/ACCESS.2019.2927760.

Chen, J. (2012): New alternating direction implicit finite-difference time-domain method with higher efficiency. *Applied Computational Electromagnetics Society Journal*, vol. 27, no. 11, pp. 903-907.

Chen, L. (2010): A new class of high order finite volume methods for second order elliptic equations. *SIAM Journal on Numerical Analysis*, vol. 47, no. 6, pp. 4021-4043. DOI 10.1137/080720164.

Chen, Z.; Wu, J.; Xu, Y. (2012): Higher-order finite volume methods for elliptic boundary value problems. *Advances in Computational Mathematics*, vol. 37, no. 2, pp. 191-253. DOI 10.1007/s10444-011-9201-8.

Dai, W.; Nassar, R. (1999): A finite difference scheme for solving the heat transport equation at the microscale. *Numerical Methods for Partial Differential Equations: An International Journal*, vol. 15, no. 6, pp. 697-708. DOI 10.1002/(SICI)1098-2426 (199911)15:6<697:AID-NUM6>3.0.CO;2-#.

De Angelis, M. (2019): A wave equation perturbed by viscous terms: fast and slow times diffusion effects in a neumann problem. *Ricerche di Matematica*, vol. 68, no. 1, pp. 237-252. DOI 10.1007/s11587-018-0400-1.

Deng, D. (2018): Unified compact adi methods for solving nonlinear viscous and nonviscous wave equations. *Chinese Journal of Physics*, vol. 56, no. 6, pp. 2897-2915. DOI 10.1016/j.cjph.2018.09.025.

Deng, S.; Wang, W.; Zhao, H. (2010): Existence theory and lp estimates for the solution of nonlinear viscous wave equation. *Nonlinear Analysis: Real World Applications*, vol. 11, no. 5, pp. 4404-4414. DOI 10.1016/j.nonrwa.2010.05.024.

Douglas, J., Jr (1955): On the numerical integration of $\frac{\partial^2 u}{\partial x^2}+\frac{\partial^2 u}{\partial y^2}=\frac{\partial u}{\partial t}$ by implicit methods. *Journal of the Society for Industrial and Applied Mathematics*, vol. 3, no. 1, pp. 42-65. DOI 10.1137/0103004.

Ewing, R. E.; Lin, T.; Lin, Y. (2002): On the accuracy of the finite volume element method based on piecewise linear polynomials. *SIAM Journal on Numerical Analysis*, vol. 39, no. 6, pp. 1865-1888. DOI 10.1137/S0036142900368873.

Gao, G. H.; Sun, Z. Z. (2016): Two alternating direction implicit difference schemes for solving the two-dimensional time distributed-order wave equations. *Journal of Scientific Computing*, vol. 69, no. 2, pp. 506-531. DOI 10.1007/s10915-016-0208-7.

Ge, Y.; Tian, Z. F.; Zhang, J. (2013): An exponential high-order compact adi method for 3D unsteady convection-diffusion problems. *Numerical Methods for Partial Differential Equations*, vol. 29, no. 1, pp. 186-205. DOI 10.1002/num.21705.

Harfash, A. J. (2008): High accuracy finite difference scheme for three-dimensional microscale heat equation. *Journal of Computational and Applied Mathematics*, vol. 220, no. 1-2, pp. 335-346. DOI 10.1016/j.cam.2007.08.010.

Karaa, S. (2006): A high-order compact ADI method for solving three-dimensional unsteady convection-diffusion problems. *Numerical Methods for Partial Differential Equations: An International Journal*, vol. 22, no. 4, pp. 983-993. DOI 10.1002/num.20134.

Karaa, S. (2009): A high-order ADI method for parabolic problems with variable coefficients. *International Journal of Computer Mathematics*, vol. 86, no. 1, pp. 109-120. DOI 10.1080/00207160802217227.

Karaa, S. (2010a): Approximate factorization for a viscous wave equation. *Computing*, vol. 89, no. 3-4, pp. 199-215. DOI 10.1007/s00607-010-0102-3.

Karaa, S. (2010b): Unconditionally stable ADI scheme of higher-order for linear hyperbolic equations. *International Journal of Computer Mathematics*, vol. 87, no. 13, pp. 3030-3038. DOI 10.1080/00207160902878548.

Karaa, S.; Zhang, J. (2004): High order ADI method for solving unsteady convection-diffusion problems. *Journal of Computational Physics*, vol. 198, no. 1, pp. 1-9. DOI 10.1016/j.jcp.2004.01.002.

Khelghati, A.; Baghaei, K. (2018): Blow-up phenomena for a class of fourth-order nonlinear wave equations with a viscous damping term. *Mathematical Methods in the Applied Sciences*, vol. 41, no. 2, pp. 490-494.

Koutserimpas, T. T.; Papadopoulos, A. D.; Glytsis, E. N. (2017): Applicability and optimization of the alternating-direction-implicit iterative method for the 2-d finite-difference frequency-domain solution of scattering problems. *IEEE Transactions on Antennas and Propagation*, vol. 65, no. 12, pp. 7166-7173. DOI 10.1109/TAP.2017.2759901.

Li, K.; Liao, W.; Lin, Y. (2019): A compact high order alternating direction implicit method for three-dimensional acoustic wave equation with variable coefficient. *Journal of Computational and Applied Mathematics*, vol. 361, pp. 113-129. DOI 10.1016/j.cam.2019.04.013.

Li, R.; Li, J.; He, X.; Chen, Z. (2018): A stabilized finite volume element method for a coupled stokes-darcy problem. *Applied Numerical Mathematics*, vol. 133, pp. 2-24. DOI 10.1016/j.apnum.2017.09.013.

Lim, H.; Kim, S.; Douglas, J. J. (2007): Numerical methods for viscous and nonviscous wave equations. *Applied Numerical Mathematics*, vol. 57, no. 2, pp. 194-212. DOI 10.1016/j.apnum.2006.02.004.

Liu, Z.; Liu, F.; Zeng, F. (2019): An alternating direction implicit spectral method for solving two dimensional multi-term time fractional mixed diffusion and diffusion-wave equations. *Applied Numerical Mathematics*, vol. 136, pp. 139-151. DOI 10.1016/j.apnum.2018.10.005.

Luo, X.; Chen, Y.; Huang, Y. (2013): Some error estimates of finite volume element approximation for elliptic optimal control problems. *International Journal of Numerical Analysis & Modeling*, vol. 10, no. 3, pp. 697-711.

Luo, X.; Chen, Y.; Huang, Y.; Hou, T. (2014): Some error estimates of finite volume element method for parabolic optimal control problems. *Optimal Control Applications and Methods*, vol. 35, no. 2, pp. 145-165. DOI 10.1002/oca.2059.

Luo, Z. (2014): A new finite volume element formulation for the non-stationary Navier-Stokes equations. *Advances in Applied Mathematics and Mechanics*, vol. 6, no. 5, pp. 615-636. DOI 10.4208/aamm.2013.m83.

Plexousakis, M.; Zouraris, G. E. (2004): On the construction and analysis of high order locally conservative finite volume-type methods for one-dimensional elliptic problems.

SIAM Journal on Numerical Analysis, vol. 42, no. 3, pp. 1226-1260. DOI 10.1137/S0036142902406302.

Qiao, L.; Xu, D. (2018): Compact alternating direction implicit scheme for integro-differential equations of parabolic type. *Journal of Scientific Computing*, vol. 76, no. 1, pp. 565-582. DOI 10.1007/s10915-017-0630-5.

Qiao, L.; Xu, D.; Wang, Z. (2019): An ADI difference scheme based on fractional trapezoidal rule for fractional integro-differential equation with a weakly singular kernel. *Applied Mathematics and Computation*, vol. 354, pp. 103-114. DOI 10.1016/j.amc.2019.02.022.

Li, R. H.; Chen, Z. Y.; Wu, W. (1999): *Generalized difference methods for differential equations: numerical analysis of finite volume methods*. New York: Mareee Dekker.

Sei, A.; Symes, W. (1995): Dispersion analysis of numerical wave propagation and its computational consequences. *Journal of Scientific Computing*, vol. 10, no. 1, pp. 1-27. DOI 10.1007/BF02087959.

Verwer, J. G. (2009): Runge-Kutta methods and viscous wave equations. *Numerische Mathematik*, vol. 112, no. 3, pp. 485-507. DOI 10.1007/s00211-009-0211-0.

Vong, S.; Wang, Z. (2015): A compact ADI scheme for the two dimensional time fractional diffusion-wave equation in polar coordinates. *Numerical Methods for Partial Differential Equations*, vol. 31, no. 5, pp. 1692-1712. DOI 10.1002/num.21976.

Wang, H.; Zhao, W. (2003): An upwind finite volume scheme and its maximum-principle-preserving ADI splitting for unsteady-state advection-diffusion equations. *Numerical Methods for Partial Differential Equations: An International Journal*, vol. 19, no. 2, pp. 211-226. DOI 10.1002/num.10044.

Wang, Q.; Zhang, Z. (2019): A stabilized immersed finite volume element method for elliptic interface problems. *Applied Numerical Mathematics*, vol. 143, pp. 75-87. DOI 10.1016/j.apnum.2019.03.010.

Wang, T. (2008): Alternating direction finite volume element methods for 2D parabolic partial differential equations. *Numerical Methods for Partial Differential Equations: An International Journal*, vol. 24, no. 1, pp. 24-40. DOI 10.1002/num.20224.

Wei, Z.; Li, C.; Zhao, S. (2018): A spatially second order alternating direction implicit (ADI) method for solving three dimensional parabolic interface problems. *Computers & Mathematics with Applications*, vol. 75, no. 6, pp. 2173-2192. DOI 10.1016/j.camwa.2017.06.037.

Yang, M.; Chen, C. (2009): ADI quadratic finite volume element methods for second order hyperbolic problems. *Journal of Applied Mathematics and Computing*, vol. 31, no. 1-2, pp. 395-411. DOI 10.1007/s12190-008-0220-7.

Zampieri, E.; Pavarino, L. F. (2006): Implicit spectral element methods and Neumann-Neumann preconditioners for acoustic waves. *Computer Methods in Applied Mechanics and Engineering*, vol. 195, no. 19-22, pp. 2649-2673. DOI 10.1016/j.cma.2005.06.005.

Zhang, J.; Zhao, J. J. (2001): Unconditionally stable finite difference scheme and iterative solution of 2D microscale heat transport equation. *Journal of Computational Physics*, vol. 170, no. 1, pp. 261-275. DOI 10.1006/jcph.2001.6735.

Zhang, Z. (2011): The multistep finite difference fractional steps method for a class of viscous wave equations. *Mathematical Methods in the Applied Sciences*, vol. 34, no. 4, pp. 442-454. DOI 10.1002/mma.1343.

Zhang, Z.; Deng, D. (2007): A new alternating-direction finite element method for hyperbolic equation. *Numerical Methods for Partial Differential Equations: An International Journal*, vol. 23, no. 6, pp. 1530-1559. DOI 10.1002/num.20240.

Zhang, Z.; Wang, T. (2004): The alternating group explicit parallel algorithms for convection dominated diffusion problem of variable coefficient. *International Journal of Computer Mathematics*, vol. 81, no. 7, pp. 823-834. DOI 10.1080/00207160410001708797.

Zhao, S. (2015): A matched alternating direction implicit (ADI) method for solving the heat equation with interfaces. *Journal of Scientific Computing*, vol. 63, no. 1, pp. 118-137. DOI 10.1007/s10915-014-9887-0.

Zhao, W.; Liu, W. (2018): A note on blow-up of solutions for a class of fourth-order wave equation with viscous damping term. *Applicable Analysis*, vol. 97, no. 9, pp. 1496-1504. DOI 10.1080/00036811.2017.1313410.

Zhao, X.; Chen, Y.; Gao, Y.; Yu, C.; Li, Y. (2013): Finite volume element methods for nonequilibrium radiation diffusion equations. *International Journal for Numerical Methods in Fluids*, vol. 73, no. 12, pp. 1059-1080.

Zhou, J.; Xu, D. (2020): Alternating direction implicit difference scheme for the multi-term time-fractional integro-differential equation with a weakly singular kernel. *Computers & Mathematics with Applications*, vol. 79, no. 2, pp. 244-255.